

UNCLASSIFIED

AD NUMBER

AD824924

LIMITATION CHANGES

TO:

Approved for public release; distribution is unlimited. Document partially illegible.

FROM:

Distribution authorized to U.S. Gov't. agencies and their contractors; Critical Technology; DEC 1967. Other requests shall be referred to Defense Advanced Research Projects Agency, Technical Information Office, Washington, DC 20301. Document partially illegible. This document contains export-controlled technical data.

AUTHORITY

arpa ltr, 18 jan 1972

THIS PAGE IS UNCLASSIFIED

AD824924

STATEMENT #2 UNCLASSIFIED

This document is subject to special export controls and each transmittal to foreign governments or foreign nationals may be made only with prior approval of

*Advanced Research Projects Agency, attn: Technical Information Office  
Washington, D.C. 20301*

Microstructure, Creep and Failure: A Program for Graduate Education and Research in High Temperature Materials

Carnegie-Mellon University  
The University of Pittsburgh  
Westinghouse Electric Corporation

The First Semi-Annual Report

December 30, 1967

ARPA Order 981, Program Code 7D10  
Contract DAHC15-67-C-0176

Westinghouse Electric Corporation  
D. R. Hamilton  
Phone (412) 256-3535

~~Reproduction or distribution of this part is prohibited by law.~~  
~~Violation of the law is a criminal offense.~~  
~~Penalties of imprisonment and/or fine.~~



**BEST  
AVAILABLE COPY**

Microstructure, Creep and Failure: A Program for  
Graduate Education and Research in High  
Temperature Materials

Carnegie-Mellon University  
The University of Pittsburgh  
Westinghouse Electric Corporation

The First Semi-Annual Report

December 30, 1967

ARPA Order 981, Program Code 7D10  
Contract DAHC15-67-C-0176

Westinghouse Electric Corporation  
D. R. Hamilton  
Phone (412) 256-3535

Reproduction in whole or part is permitted for  
any purpose of the United States Government.  
Distribution of this document is unlimited.

## Table of Contents

	<u>Page</u>
Introduction.....	1
Calendar of Events.....	3
1. Mechanical Properties of Unidirectionally Solidified Ni-Cr Eutectic..... R. Kossowsky, W. C. Johnston and B. J. Shaw	4
2. Solidification Studies..... H. D. Brody	39
3. The Effect of Microstructure on the Behavior of Nickel- Chromium Alloys under Conditions of Thermal Shock.... R. D. Townsend	48
4. Low-Cycle Fatigue of Niobium Single Crystals..... J. C. DiPrimio	50
5. Fatigue of Metals in a Vacuum Environment..... H. F. Andrasik	53
6. Mechanical Properties of Fine-grained, Low Porosity Ceramics..... M. Papapietro and D. Ragone	57
7. Solid Solution and Precipitation Hardening of Oxides... J. S. Foster	59
8. Properties of Refractory Metals Carbides..... J. S. Foster	62
9. Screening of Eutectic Combinations: Cobalt Base, Aluminum Base and Silver-Silicon..... R. Kossowsky, W. C. Johnston and B. J. Shaw	64

### Abstract

The three major sections of this report are eutectics, metal fatigue and ceramics, and the research in these is spread across the Carnegie-Mellon University, the University of Pittsburgh and the Westinghouse Research Center. Whereas the majority of the projects are in formative stages, the work on the nickel-chromium eutectic is well developed. It covers the solidification under various growth conditions and the resultant mechanical properties over the temperature range -250 to 850°C. The composite strength is analyzed in terms of the rule of mixtures. Experimental studies of the stability of the lamellar microstructure of NiCr during growth are being done in an EB float zone apparatus. Two sets of fatigue experiments are underway, and those on low cycle fatigue in ultrahigh vacuum have reached the apparatus testing stage. In ceramics, the experimental work is furthest along in MgO and its alloys, with mechanical tests and electron microscopy of TiC almost as far advanced.

**BLANK PAGE**

## Introduction

This is the first semi-annual report on the ARPA contract DAHC15-67-C-0176, and for the most of the participants, many of whom have just arrived, it represents an "equipment and material organization" stage at which few experimental results are available. Work on the mechanical properties of the nickel-chromium eutectic is an exception and a start has been made on the growth characteristics of this material in an electron beam zone refiner.

The report has been arranged in order of subject rather than location so that projects of a similar nature may appear together.

Dr. B. J. Shaw, Dr. W. C. Johnston and Dr. R. Kossowsky at Westinghouse Research, Dr. H. D. Brody at the University of Pittsburgh and Dr. R. D. Townsend at the Carnegie-Mellon University are working on the solidification and mechanical properties of the Ni-Cr eutectic. At the same time, Dr. R. D. Townsend shares in common with Dr. J. C. DiPrimio and Mr. H. F. Andrejasik of the University of Pittsburgh the topic of fatigue in metals. Dr. D. Ragone, Dr. M. Papapietro and Dr. J. S. Foster at the Carnegie-Mellon University are concerned with research on the mechanical properties of various ceramics.

Each investigation has been presented separately in this report, though it is anticipated that the format will change slightly with time as the authors combine in subjects of common interest. The personnel and those responsible for the contract are:

Carnegie-Mellon University

Coordinator	Professor H. Paxton
Assistant Coordinator	Dr. D. Ragona
	Dr. J. S. Foster
	Dr. M. Papapietro
	Dr. R. D. Townsend

University of Pittsburgh

Coordinator	Professor E. Salkovitz
Assistant Coordinator	Dr. H. D. Brody
	Dr. J. C. DiPrimio
	Mr. H. F. Andrejasik

Westinghouse Research & Development Center

Coordinator	Dr. D. R. Hamilton
Assistant Coordinator	Dr. B. J. Shaw
	Dr. W. C. Johnston
	Dr. R. Kossowsky

Calendar of Events

Our monthly luncheon meetings have continued during the second quarter. The following members of the ARPA contract have given short presentations at these of their area of interest and their progress, with subsequent general discussion.

<u>Place</u>	<u>Date</u>	<u>Speaker</u>	<u>Affiliation</u>
Westinghouse	September 19, 1967	Mr. P.J. Jablonski	Carnegie-Mellon
Carnegie-Mellon	October 27, 1967	Dr. W. C. Johnston Dr. H. D. Brody	Westinghouse Pittsburgh
Pittsburgh	November 21, 1967	Dr. R. Kossowsky Dr. J.S. Foster	Westinghouse Carnegie-Mellon

The following seminars have been given

Westinghouse	August 15, 1967	Mr. J.T. Smith	Lehigh University
Pittsburgh	October 3, 1967	Mr. M. Donner	Pittsburgh
Pittsburgh	December 12, 1967	Dr. N.J. Grant	M.I.T.

On November 17 graduate students made a tour of the facilities at Westinghouse Research.

1. Mechanical Properties of Unidirectionally  
Solidified Ni-Cr Eutectic

by

R. Kossowsky, W. C. Johnston and B. J. Shaw  
Westinghouse Research & Development Center

Introduction

In recent years there has been increasing interest in dispersion and second phase strengthening in materials needed for high temperature applications. The role of structure on the mechanical properties of such alloys has been well established experimentally and to some extent accounted for theoretically. The problem of how the strengthening mechanisms due to fibers and lamellae operate has been reduced to its simplest form by the fabrication of composites of strong rods unidirectionally aligned in a ductile matrix.

From work on tungsten-fiber-reinforced copper, for example, it was established that the "Rule of Mixtures" could explain the strengthening.<sup>1,2</sup> A somewhat more sophisticated technique for introducing strong fibers into copper matrix was used by Hertzberg and Kraft<sup>3</sup> who unidirectionally solidified copper-chromium eutectic. The use of unidirectionally solidified eutectics has advantages in that there are no matrix-fiber wetting problems and fine fibers are automatically aligned and uniformly spaced. However, one is restricted to a specific volume fraction of the second phase. Nevertheless, even though the volume fraction is fixed, the rod or lamella thickness  $\lambda$ , can be varied by controlling the freezing interface velocity.<sup>4</sup>

Alternatively, the grown material may be worked down by swaging or rolling. Embury and Fisher,<sup>5</sup> using this approach, drew down pearlite in iron and studied the mechanical properties. They found that the yield strength,  $\sigma_y$ , was proportional to  $d^{-1/2}$  where  $d$  was the wire diameter. It could be inferred that  $\sigma_y$  was also proportional to  $\lambda^{-1/2}$ ; but the work hardening had to be taken into consideration at the same time. By varying the growth rate of the cadmium-zinc lamellar eutectic, Shaw<sup>6</sup> showed that

$$\sigma_y \propto \lambda^{-1/2} \quad (1)$$

without the introduction of work hardening. He suggested that the lamellar interface itself contributed to the strengthening of the composite. It cannot be inferred necessarily that equation (1) is general to all composites since their properties depend on the relative strengths, orientations and physical properties of the two phases.

In this investigation we have evaluated the mechanical properties of the unidirectionally solidified fcc - bcc eutectic Ni-Cr. This eutectic was selected because it presented the possibility of a high strength, high temperature and high corrosion resistant alloy for turbine blade applications, and also represented a hard-soft phase combination with two completely different slip systems.

Specimens have been tested in compression and tension up to 850°C and a detailed study of the microstructure as a function of plastic strain and temperature has been carried out by electron microscopy. Tentative arguments indicate that the composite strength

can be interpreted in terms of the simple rule of mixtures. For lamellae of the thickness  $\lambda \sim 10$  microns produced from the melt it is shown that no strengthening is derived from the lamellar interfaces or from the lamellar size itself, in direct contrast to the results of Embury and Fisher<sup>5</sup> and Shaw.<sup>6</sup>

It is probable that the interfaces and lamellar spacing would become more dominant factors in the strength of the Ni-Cr lamellar eutectic if the structure could be made much finer. Since it has not proved possible to refine the structure by increasing the growth velocity from the melt, we are currently attempting to roll the material down in order to investigate this point.

A. Growth of the Lamellar Eutectic

Apparatus for Unidirectional Solidification

Figure 1 shows the apparatus used to produce 0.2 in. diameter samples of alloys melting up to 1500°C. The crucible tube is alumina, 5 mm I.D. x 24 in long and contains the charge which has been cast, swaged or machined to 0.195 in diameter. The lower end of the tube is immersed in a flowing water bath. The upper end is supported by a 10 mil nichrome wire which lowers the crucible and charge out of the furnace at a prescribed rate. Surrounding the crucible is a graphite susceptor into which a control thermocouple is inserted. The furnace is insulated with fiberfrax and enclosed in a quartz tube. There is a sliding seal at the bottom around the crucible and one on the top so that an atmosphere may

be used for the sample and susceptor. The power for this furnace is supplied from a 10 kw, 450 kc generator.

Figure 2 shows the apparatus used to produce bars from 3/8 in. diameter up to 1-1/2 in diameter. It is similar in operation to 0.2 in. diameter size but uses a 10 kc source. The control thermocouple is again inserted within the wall of the susceptor but there is sufficient space within the furnace to install thermocouples in the sample. Crucible tubes of which the internal diameters are 3/8 in and 1/2 in respectively very seldom cracked during a run. However, for the 1-1/2 in diameter size, special precautions were taken and a unique design evolved.

The sample is placed in the crucible tube in two pieces with an expansion gap between the two located at the intended molten zone position. The top piece is pinned to the crucible. Molybdenum rods also hold the top and bottom parts of the crucible together. Thus if the crucible develops a crack the molybdenum rods will prevent the crucible from separating into two pieces with subsequent loss of the liquid zone.

The skin depth for graphite ( $\rho = 10^7 \mu\text{-ohm-cm}$ ) is 1.15 in at these frequencies and the actual wall thickness is 3/8 in. The field thus penetrates the susceptor and induces currents in the melt which stir the melt, controlling both solute and heat transport at the interface. Thermocouple measurements in the melt indicate a liquid zone that is completely stirred and mixed. Stirring is controlled by changing the thickness of the susceptor.

Results

Temperature gradients in the sample were measured in the large experimental apparatus. The temperature gradient was controlled by adjusting the temperature of the graphite susceptor (see Fig. 2). The gradient was measured by inserting a tungsten-tungsten 26% rhenium thermocouple and sheath into the melt and taking a time temperature traverse during freezing. In this manner the temperature profile in the molten zone and during the freezing could be measured. The temperature gradient ranged from about  $100^{\circ}\text{C/in}$  to  $300^{\circ}\text{C/in}$ .

The stability of the interface depends upon the temperature gradient, the growth velocity, and the purity of the sample materials.<sup>7</sup> Analysis of three samples of the NiCr are given in Table I. The first is for material cast at Westinghouse and the latter two for material received from Leytess before and after the crystal was grown. With the exception of Fe, Mn and Co, the three analyses are about the same. It is concluded that very little partitioning is taking place, and very little impurities are picked up from the crucible (99.9% pure alumina).

The characteristics of the growth are shown in Fig. 3, where temperature gradient is plotted against growth velocity. The area to the left and above the line is the region of stable lamellar growth. A photomicrograph of run T-13 in this stable region is shown in Fig. 4, where 4(a) is a transverse section showing complete lamellar filling of the entire cross-section. The growth rate was  $1/3$  in/hr, the temperature gradient  $160^{\circ}\text{C/in}$ , and the lamellar spacing 15 microns. Even though

there are quite a few grains in a cross section (1/2 in diameter) the lamellae from one grain to another show some degree of coordination. Figure 4(b) is a longitudinal section of run T-13 showing that the lamellae are continuous.

In Fig. 3 the area to the right and below the line is a region of cellular and dendritic growth. Figure 5(a) is a transverse section of run T-17 showing the growth of dendrites with lamellae and rods filling the space in between. The growth rate was 1 in/hr and the temperature gradient  $160^{\circ}\text{C}/\text{in}$ . Figure 5(b) shows a photomicrograph of run T-12 made at 2 in/hr. There are more dendrites and rods and less lamellae.

A range of growth rates from 0.1 in/hr to 8 in/hr was investigated to determine the extent of stable interfaces. It was found that above 1 in/hr the interface became unstable and dendritic growth developed, while speeds below 0.1 in/hr are impractical, so that the growth range is about 10 to 1. It has been shown<sup>4</sup> that the lamellar spacing varies as the inverse root of the growth velocity. The lamellar spacing was measured on samples and is shown in Fig. 6. The smallest spacing is about 5 microns. In order to determine role of the interface upon the mechanical properties, it is necessary to either grow, or in some way produce, material with a finer lamellar spacing. Finer lamellar spacing would require growing at a faster speed which invariably produces dendrites.

An attempt was made to reduce the lamellar spacing by hot swaging a bar of grown material. One-half inch grown bars of material at  $1000^{\circ}\text{C}$  were swaged to a size of  $1/4$  in diameter in steps with reheating in between

operations. Cracks began to develop and samples were cut from the bar. It was found that the lamellae were twisted and folded upon each other and internal cracks were developing. It was concluded that hot rolling would have a better chance of success.

Samples of grown material were encapsulated in stainless steel cylinders for the purpose of hot rolling. The space between the sample and the cylinder was filled with alumina powder. Reductions of 50% have been made at 900°C and the material has been examined. Apart from normal surface cracks on the rolled ingot, no internal cracks were found. In some areas, lamellar refinement was found thus indicating that the technique may be successful.

During the freezing process there is a redistribution of the chromium and nickel. The composition freezing out in the matrix and in either the lamellae or rods is indicated on the phase diagram shown in Fig. 7. However, as the sample cools down, nickel in the lamellae or rods must either precipitate or diffuse out, and likewise the matrix is capable of accepting more nickel in solution. Figure 8 shows a microprobe trace of the nickel and chromium content of a sample which contained both lamellae and rods. It is seen that the nickel content in the lamellae and rods is quite a bit lower than the equilibrium value for the eutectic temperature. Furthermore, the nickel content in the matrix has increased showing that nickel is diffusing out of the lamellae and rods into the matrix. In Fig. 8 it can be seen that the

concentration gradients in the lamellae and rods are very steep. The final composition of the samples corresponds to an upper equilibrium temperature of about 1150°C.

Table I

Analysis of material from Leytess as received (L-1B) and after growing (L-1A) with Westinghouse nominal 99.9% after growing (VM964), in wt %.

	Ni	Cr	P	Mg	C	S	N	O
L-1B	49.0	50.6	< 0.0005	< 0.003	0.0103	0.0010	0.0030	0.019
L-1A	48.9	50.7	< 0.0005	< 0.003	0.0126	0.6010	0.0022	0.016
VM964	47.5	52.2	< 0.0005	< 0.003	0.0075	0.6010	0.0065	0.033
	Fe	V	Mn	Ti	Mo	Co	Cn	Si
L-1B	0.006	< 0.001	< 0.001	< 0.001	< 0.001	< 0.001	< 0.001	< 0.001
L-1A	0.006	< 0.001	< 0.001	< 0.001	< 0.001	< 0.001	< 0.001	< 0.001
VM964	0.1	< .001	0.05		.005	< .001	0.02	< .001
								0.02

B. Electron Microscopy and Mechanical Testing

Electron Microscopy

Specimens for the electron microscope were prepared by wafering blanks from the as grown and from the tested specimens perpendicular to the growth direction. The blanks were ground to .25 mm thickness on a fine emery paper then further reduced to .13 mm by polishing with  $1\mu$  diamond paste. Final polishing was performed in an automated jet polisher. The fact that the alloy is composed of two distinct phases caused some difficulties in electropolishing. A given electrolyte designed to polish one phase would cause the other to polish at a different rate. Consequently, one phase, generally the nickel, was polished until first

perforation occurred. The hole was then masked and polishing was resumed in another solution. Polishing conditions were as follows:

Ni rich phase, 23 ml perchloric acid and 77 ml glacial acetic acid, at 25-30V and  $0.7 \text{ A/cm}^2$ .

Cr rich phase, 420 ml phosphoric (85%) acid, 340 ml sulfuric acid and 240 ml water at 2.8 V and  $0.1-0.2 \text{ A/cm}^2$ .

All specimens were studied in a JEM-7 electron microscope operating at 100 kV.

### Results

Figure 9 is a typical electron micrograph of the as-grown structure with the typical grown in dislocation density. Two features should be emphasized. The lack of dislocation concentration or pile-ups at the Cr-Ni boundaries, indicating no residual growth stress, and the internal structure in the Cr rich lamellae. This structure is shown at a higher magnification in Fig. 10 and was identified by electron diffraction primarily as  $\text{Cr}_2\text{O}_3$ . Diffraction patterns, taken simultaneously of both phases yielded the following relations:

$$(211) \text{ Ni} \parallel (1\bar{1}0) \text{ Cr}$$

and

$$[1\bar{1}\bar{1}] \text{ Ni} \parallel [1\bar{1}0] \text{ Cr}$$

Mechanical properties were primarily investigated by means of compression testing at temperatures between -198 and  $850^\circ\text{C}$  for both as grown, swaged and annealed specimens, as shown in Fig. 11. Also included in Fig. 11 are three tensile tests. The curves for the grown and swaged specimens are displaced by a constant stress of about 105,000 psi.

Above 500°C the effect of swaging is diminishing and disappears at 860°C. Also note that as temperature increases the difference between compression and tensile strength decreases. Added to Fig. 11 are microhardness test results which have a bearing upon the deformation characteristics of the two phases. In the as-grown condition the chromium rich phase is twice as hard as the nickel rich phase. After 40% cold reduction, followed by half an hour anneal at 1000°C, the chromium rich phase has work hardened by an insignificant amount, while the hardness of the nickel rich phase has almost doubled.

Figures 12 to 15 are light micrographs of tensile specimens deformed at temperatures between 20 and 1080°C. At room temperature (Fig. 12) the chromium rich phase fractures in a typical brittle manner while the failure of the more ductile nickel rich phase is delayed. At 500°C (Fig. 13) the chromium rich phase exhibits some ductility and one can observe the bending of the lamellae along the maximum shear direction at 45° to the tensile axis. Increased ductility of the chromium rich phase is seen in Fig. 14, which is a light micrograph of a specimen deformed at 800°C. At 1080°C (Fig. 15) this phase is very ductile. One also observed a large number of voids formed at the interface, also reported in fcc aluminum<sup>8</sup> and bcc tantalum,<sup>9</sup> both of which had large numbers of inclusions.

The dislocation structures in deformed specimens are illustrated in Figs. 16 to 18. Two percent deformation at room temperature (Fig. 16a) results in band structure typical for fcc alloys with low stacking fault energy, such as Cu-7.5 A% Al,<sup>10</sup> 18-8 stainless steel and Ni-19Cr

superalloy,<sup>11</sup> which deform at the early stages by planar slip. Although the stacking fault energy of pure nickel is rather high,<sup>12</sup> of the order of 150 erg/cm<sup>2</sup>, the addition of chromium lowers it to about 25 erg/cm<sup>2</sup>. After 40% RA by cold swaging followed by 1/2 an hour anneal at 1000°C, a definite sub-structure has developed (Fig. 16b) which shows ring diffraction patterns typical of a polycrystalline material. Deformation at high temperature (Fig. 17) is characterized by an irregular tangled dislocation structure with occasional nickel oxide particles. The structure of the Ni-Cr interphase boundary following room temperature deformation is shown in Fig. 18 where one can observe a narrow band of tangled dislocations running vertically at the left third of the figure. The structure inside the chromium rich phase is somewhat difficult to resolve but does not seem to be significantly different from that in the as-grown material, Fig. 10.

#### Discussion

If one assumes a complete load transfer across the interface of a two-phase material such as a unidirectionally solidified Ni-Cr eutectic, then the strength of the composite  $\sigma_c$  should be given by the simple law of mixture,  $\sigma_c = \sigma_{Cr} V_{Cr} + \sigma_{Ni} (1 - V_{Cr})$ . Table II summarizes three tensile test results (Fig. 11) and calculated strengths for the composite, assuming 21% for  $V_{Cr}$ , the volume fraction of the chromium rich phase.

Table II

Test Temp. (°C)	$\sigma_{Ni}$ 1000 psi <sup>10</sup>	$\sigma_{Cr}$ 1000 psi <sup>10</sup>	$\sigma_c$ , calc. 1000 psi	$\sigma_c$ , measured 1000 psi
20	45	115	59	57
500	22	72	32	38
800	13	26	16	36

The values for the intrinsic strengths of Ni-Cr solid solutions were obtained from a publication by International Nickel Company<sup>16</sup> for Ni-35Cr ( $\sigma_{Ni}$ ) and Cr-15Ni ( $\sigma_{Cr}$ ), respectively (see also Fig. 8). The agreement between the measured and calculated values for  $\sigma_c$  at room temperature suggests that the strength of the composite is, in fact, controlled by the load bearing capacity of the individual phases through a load transfer across the interface. This statement also implies that each phase deforms independently of the other. Additional support to this hypothesis is found by studying the many electron micrographs. Evidence of dislocation pile-ups at the interphase boundaries<sup>13,14</sup> could not be found. Furthermore, Fig. 16a shows that the nickel rich phase is deforming in a manner typical of a single phase fcc alloy<sup>11</sup> with a low stacking fault energy. Comparing Fig. 18 with Fig. 9 one can observe a narrow band of dense dislocation at the interphase boundary of the deformed specimen indicating the development of shear stresses across the interface.

The test results at 500°C and 800°C (Table II), however, are certainly not compatible with the law of mixtures. Possibly the values of  $\sigma_{Cr}$  taken from the literature<sup>16</sup> are lower than the actual strength of our thin chromium lamellae with their embedded oxide particles. Obviously, a more rigorous analysis will be possible after we have secured independent data for the deformation characteristics of the two individual phases.

Bearing this in mind, it is possible to account, at least qualitatively, for the various features of Fig. 11. The chromium rich phase is the harder, less ductile of the two. As load is applied it does not deform plastically to any appreciable extent (no change in hardness) whereas the nickel rich phase does deform plastically and work hardens. Due to its brittleness (Fig. 12) the chromium rich phase can sustain higher loads in compression, which probably accounts for much of the difference between tensile and compression yield strengths in as-grown material, a difference which is typical of composite materials. At higher test temperatures, the chromium rich phase exhibits some ductility (Figs. 13-15) which is consistent with the decrease with temperature of the gap between the tensile and compressive yield strengths in the as-grown material. The increase in strength of the swaged specimens is probably due to the work hardening of the nickel rich phase, for it developed a dense dislocation sub-structure after 1/2 an hour anneal at 1000°C (Fig. 16b). At temperatures above 500°C the effectiveness of the cell walls as barriers to dislocation motion surely decreases, apparently becoming ineffective at 800°C and above.

The strengthening mechanisms operating in two-phase materials have been related to dislocation pile-up at the interphase boundary,<sup>13,14</sup> to dislocation bowing<sup>15</sup> or to a modified Petch type approach.<sup>5</sup> The critical parameter in all of these approaches is the characteristic spacing between the dispersed second phase, to its particles, rods or lamellae. We did not vary this parameter in our experiments because (a) the as-grown spacing has only very recently been varied, and (b) earlier material could not be swaged to more than 40% RA. We are attempting to work the grown eutectic by hot rolling and in fact have already had some limited success. The results will be included in the next report.

Acknowledgments

We are indebted to Dr. C.J. Spengler for the x-ray microprobe analysis and to Dr. A. Noreika for continued help with the electron microscopy. At all stages of the project we were assisted by Messrs. F.C. Foust, J.E. Hudson and Mrs. Carole Muro.

References

1. D. L. McDanel, R. W. Jech and J. W. Weeton, Trans. AIME 233, 636 (1965).
2. A. Kelly, Proc. Roy. Soc. 282, 63 (1964).
3. R. W. Hertzberg and R. W. Kraft, Trans. AIME 227, 580 (1963).
4. W. A. Tiller and R. Mrdjenovich, J. Appl. Phys. 34, 3659 (1963).
5. J. D. Embury and R. M. Fisher, Acta. Met. 14, 147 (1966).
6. B. J. Shaw, Acta. Met. 15, 1169 (1967).
7. G. A. Chadwick, Eutectic Alloy Solidification, 'Progress in Material Science' Pergamon Press, Oxford, England, Vol. 12, No. 2, 1963, pp. 137.
8. G. Y. Chin, W. F. Hosford, Jr., and W. A. Backofen, Trans. Met. Soc. AIME, 230, 437 (1964).
9. R. Kossowsky, in Proceedings, 4th Symposium on Refractory Metals, French Lick, October 1965.
10. C. E. Feltner and C. Laird, Acta. Met. 15, 1633 (1967).
11. R. Kossowsky and D. M. Moon, Proceedings, Int. Conf. on Strength of Metals and Alloys, Tokyo, September 1967.
12. J. Friedel, Dislocations, Pergamon Press, New York (1964), p. 158.
13. Y. T. Chou, Acta. Met. 13, 779 (1965).
14. D. M. Barnett and A. S. Tetelman, Canad. J. Phys. 45, 841 (1967).
15. C. J. Barton and G. S. Ansell, Acta. Met. 14, 1281 (1966).
16. International Nickel Co., publication, 3M, 2-67 4456, "High Chromium, High Nickel Alloys for High Temperature Corrosion Resistance".

List of Figures

- Fig. 1 Apparatus for the unidirectional solidification of 0.2 inch diameter specimens.
- Fig. 2 Apparatus for the unidirectional solidification of 0.75 to 1.5 inch diameter specimens.
- Fig. 3 Growth characteristics of the Ni-Cr eutectic as a function of temperature gradient and velocity at the liquid-solid interface. Regular stable lamellar growth occurs above the line, in regions of high gradient.
- Fig. 4 (a) Transverse and (b) longitudinal cross sections of Ni-Cr eutectic specimen T-13.
- Fig. 5 (a) Transverse section of Ni-Cr eutectic grown at 1 in/hr, gradient 160°C/in (50X), Run T-17  
(b) Transverse section of Ni-Cr eutectic grown at 2 in/hr gradient 160°C/in (100X), Run T-13
- Fig. 6 Lamellar spacing as a function of  $(\text{velocity})^{-1/2}$  for Ni-Cr eutectic.
- Fig. 7 Ni-Cr phase diagram.
- Fig. 8 Relative x-ray intensities obtained by a scanning microprobe beam. Note the sharp gradients at the Ni-Cr interphase boundary and the dips in peak centers indicating rejection of Ni from Cr solid solution.
- Fig. 9 A typical transmission electron micrograph of an as-grown specimen, solidified at the rate of 1/3 in/hr. All subsequent specimens shown in the Figures were grown at this rate.
- Fig. 10 High magnification electron micrograph of a typical chromium rich lamella. The internal structure was identified by electron diffraction as  $\text{Cr}_2\text{O}_3$  in the main.
- Fig. 11 0.2% yield in compression and tension for as grown material as a function of test temperature, and compressive yield for 40% RA swaged material.
- Fig. 12 Light micrograph of a longitudinal section from a specimen deformed at room temperature (1000X). Note brittle failure of the chromium rich lamellae.

List of Figures (cont'd)

- Fig. 13 Light micrograph of a specimen deformed in tension at 500°C (200X)  
a: shoulder section  
b: gauge section. Note some ductility in the chromium rich lamellae.
- Fig. 14 A specimen deformed in tension at 800°C. Note increased ductility of the chromium rich phase and separation along the interphase boundary.
- Fig. 15 Shoulder and gauge sections of a specimen deformed in tension at 1080°C. The chromium rich lamellae are highly ductile and there is extensive void formation.
- Fig. 16 Transmission electron micrograph of specimens a) deformed 2% in compression. This band structure is typical of fcc alloys with low stacking fault energy, and b) swaged 40% RA, annealed 1/2 an hour at 1000°C. Note the formation of a dislocation sub-structure. The plane of foils is (211) Ni.
- Fig. 17 Transmission electron micrograph of a specimen deformed 5% at 850°C showing dislocations and some additional particles. The diffraction pattern of this area shows (211) Ni and also  $Ni_2O_3$ .
- Fig. 18 This specimen was deformed 5% in compression at room temperature. Note the narrow dislocation band at the Ni-Cr interphase boundary (arrows).

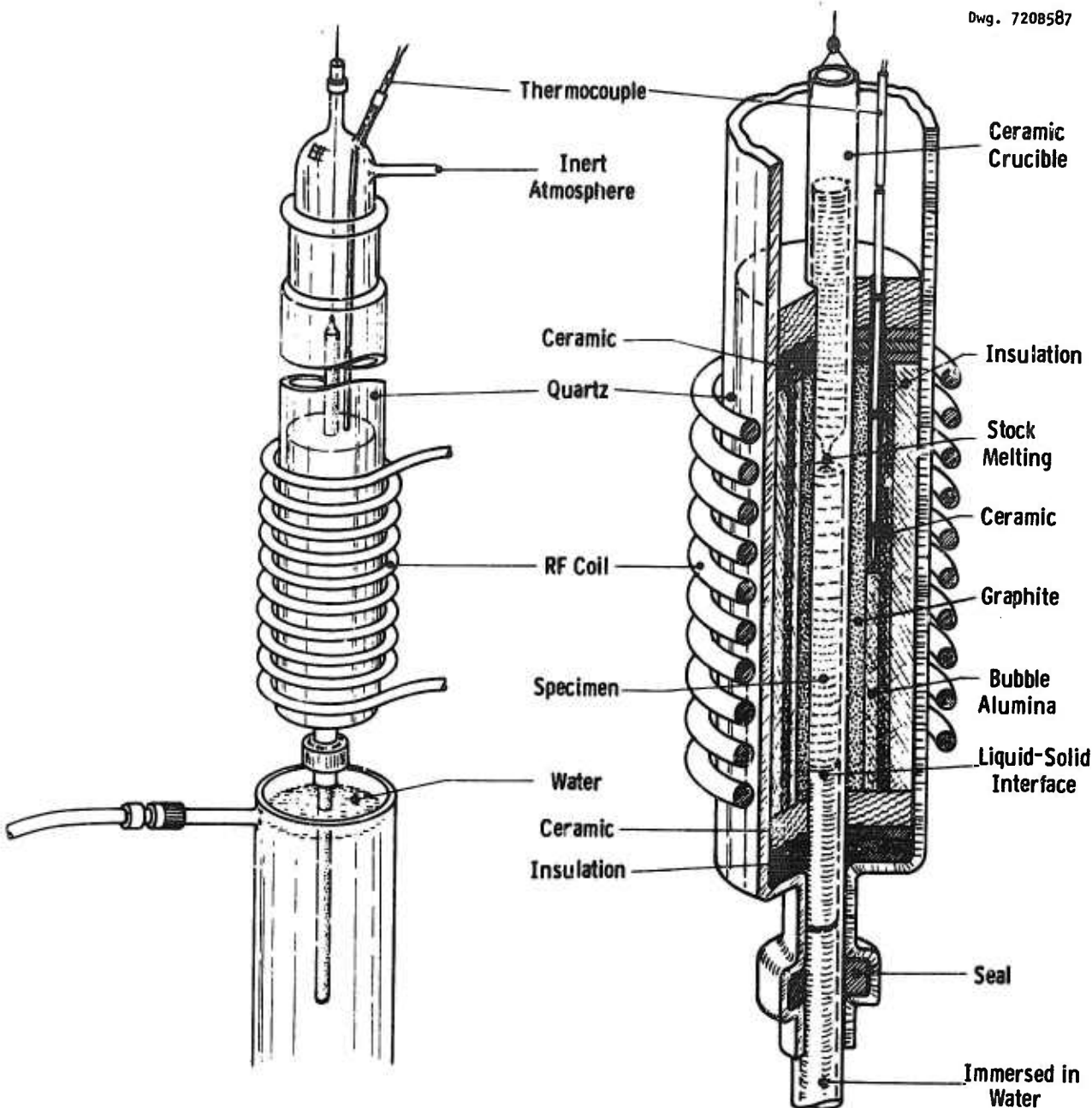


Fig. 1—Apparatus for the unidirectional solidification of 0.2 inch diameter specimens

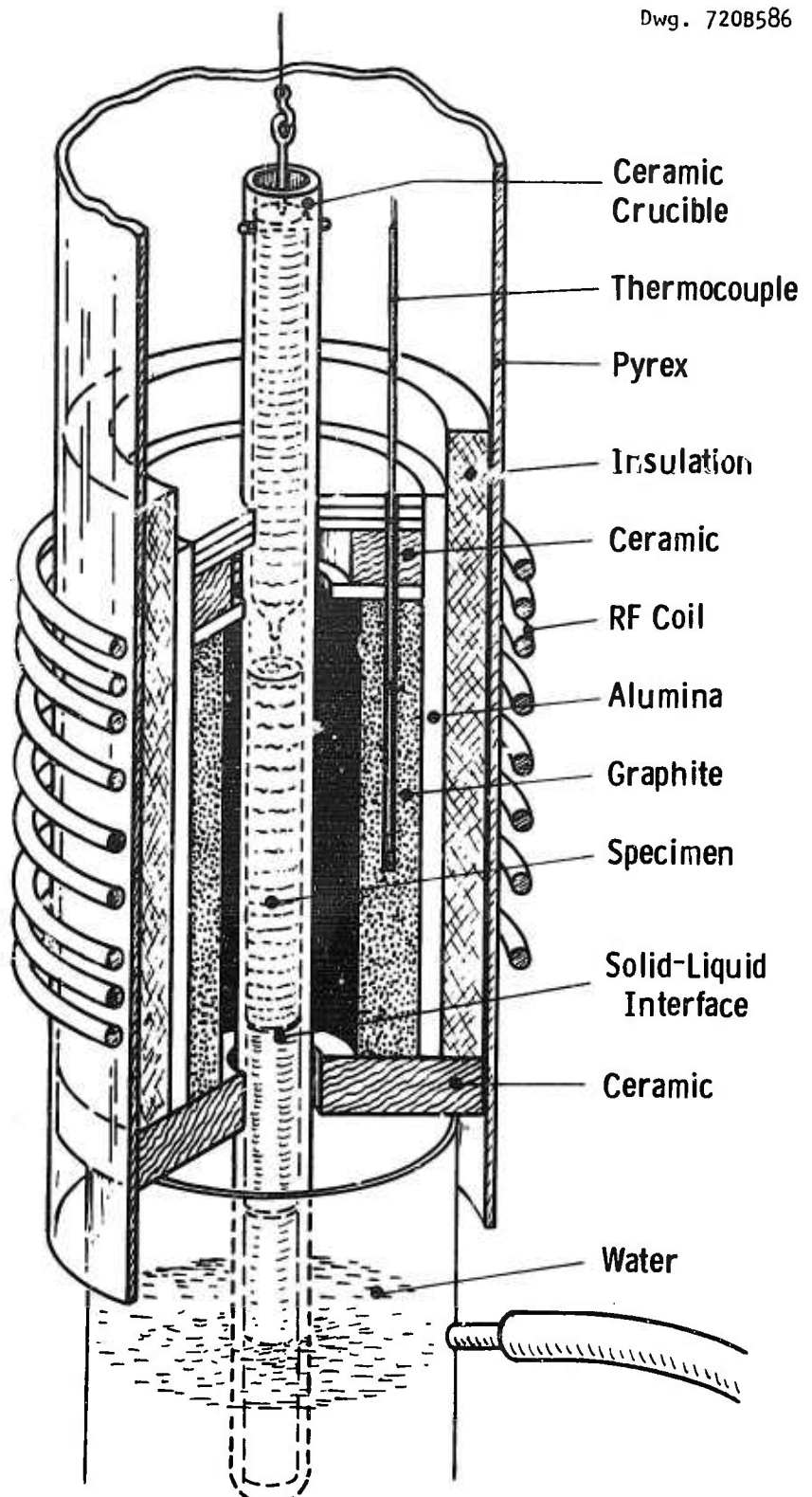


Fig. 2—Apparatus for the unidirectional solidification of 0.75 to 1.5 inch diameter specimens

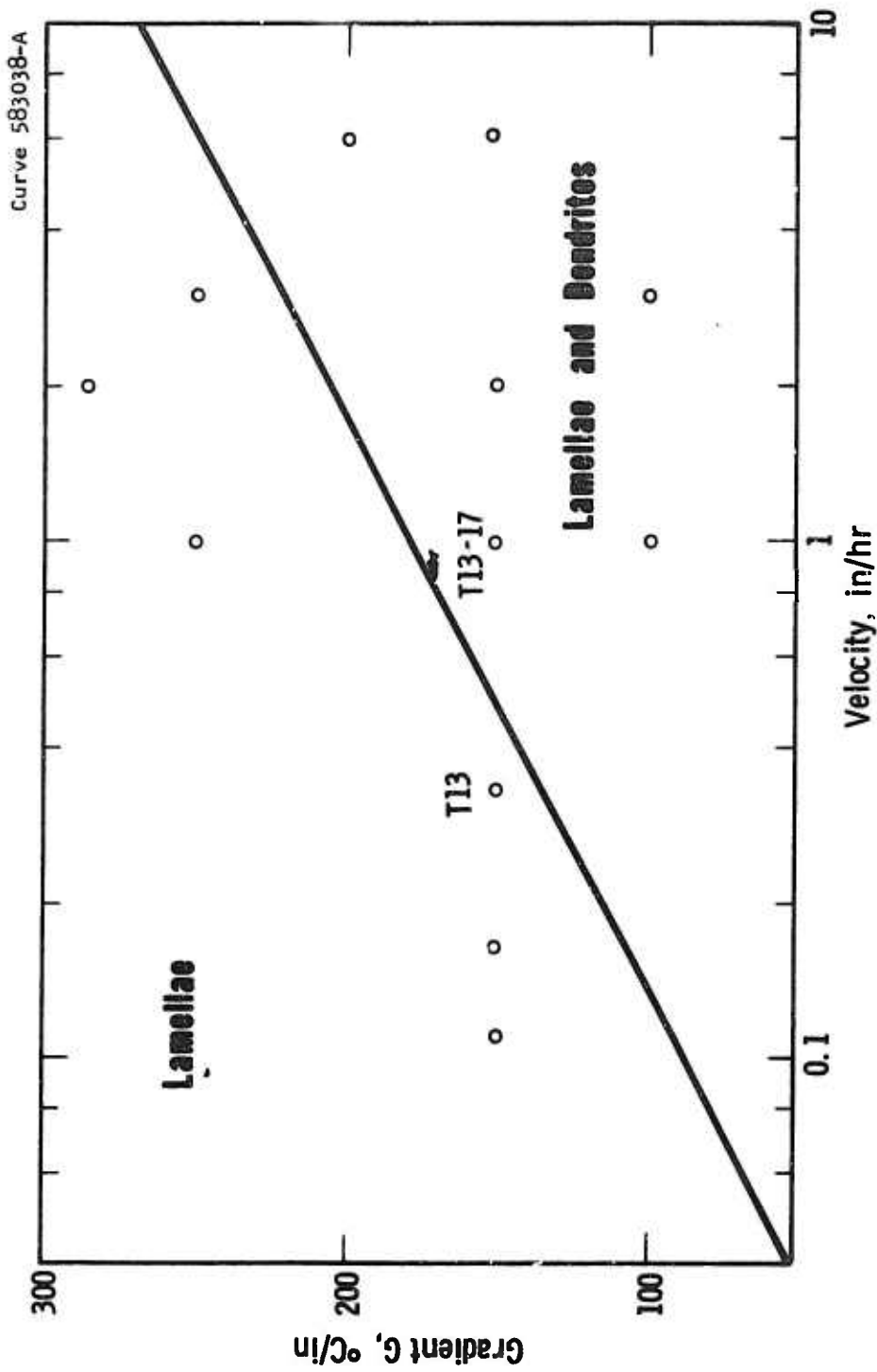
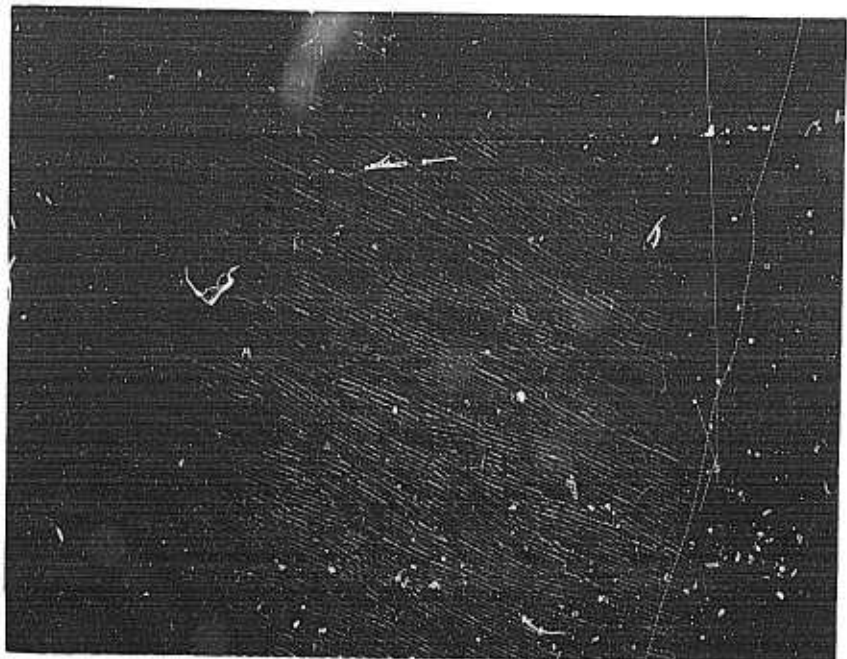
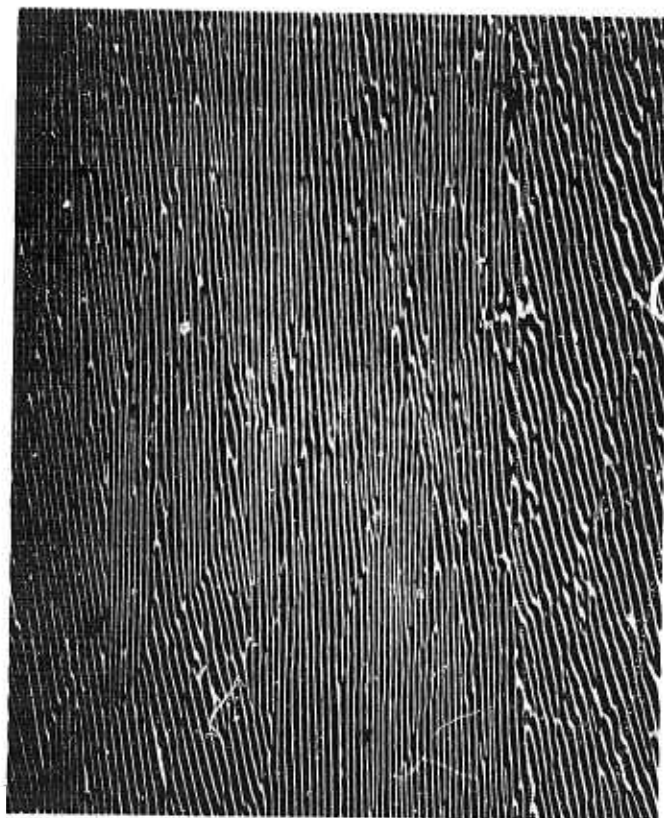


Fig. 3—Growth characteristics of the Ni-Cr eutectic as a function of temperature gradient and velocity at the liquid-solid interface. Regular stable lamellar growth occurs above the line, in regions of high gradient

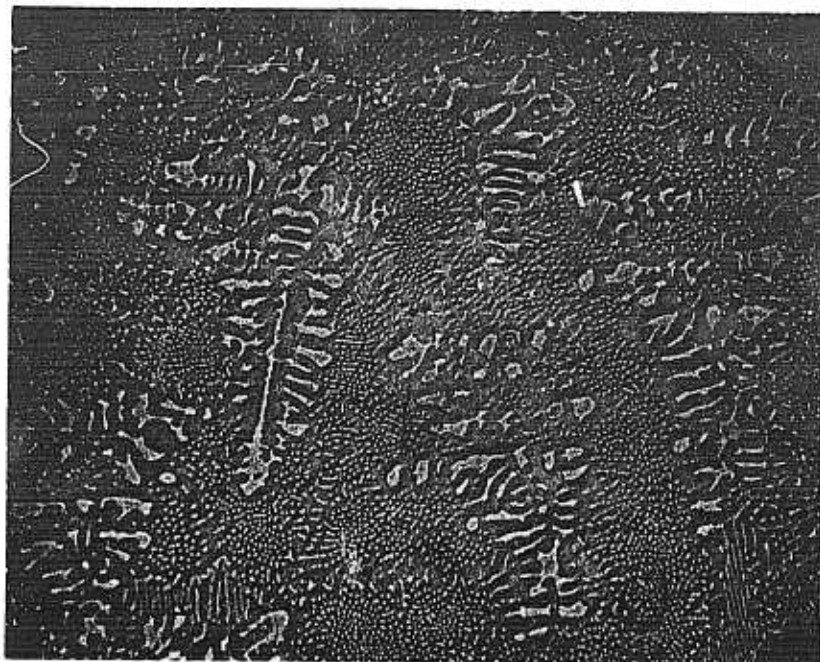


(a) Transverse 50X

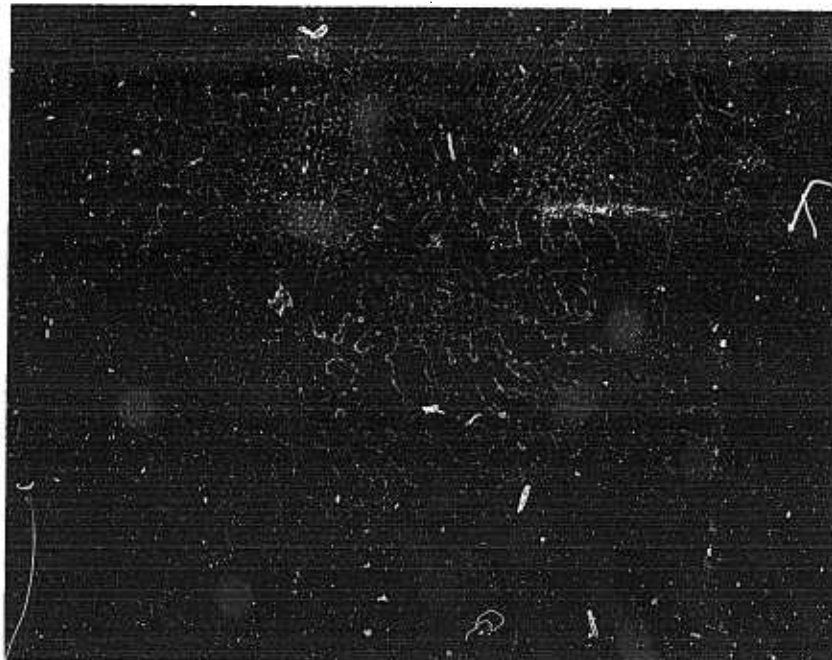


(b) Longitudinal 50X

Fig. 4-(a) Transverse and (b) longitudinal  
cross sections of Ni-Cr eutectic specimen  
T-13



(a) Transverse section of Ni-Cr Eutectic Grown  
at 1 in./hr, Gradient 160°C/in. (50X), Run T-17



(b) Transverse Section of Ni-Cr Eutectic Grown  
at 2 in./hr, Gradient 160°C/in. (100X), Run T-13

Fig. 5

Curve 583039-B

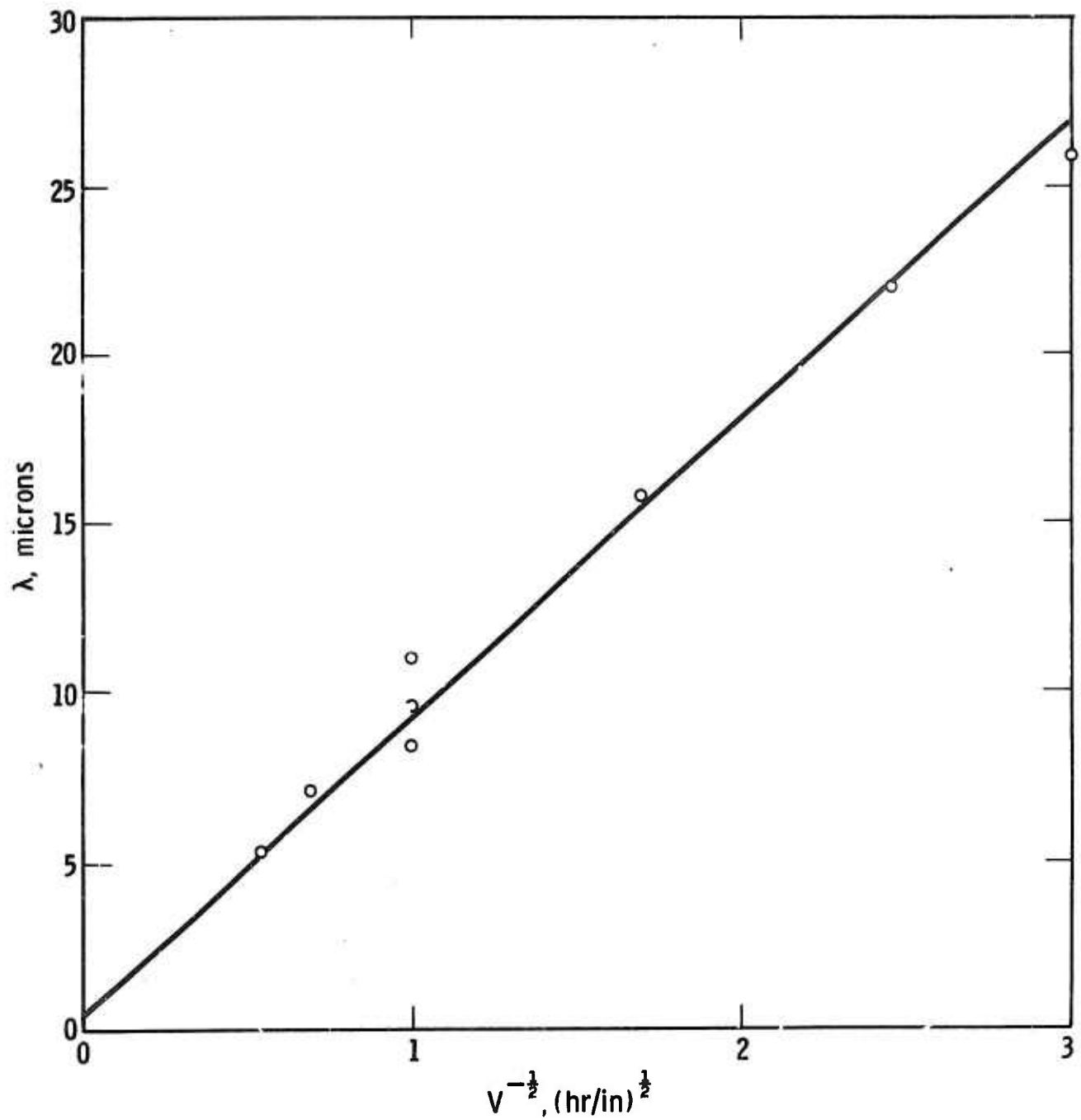


Fig. 6—Lamellar spacing as a function of  $(velocity)^{-\frac{1}{2}}$  for Ni-Cr eutectic

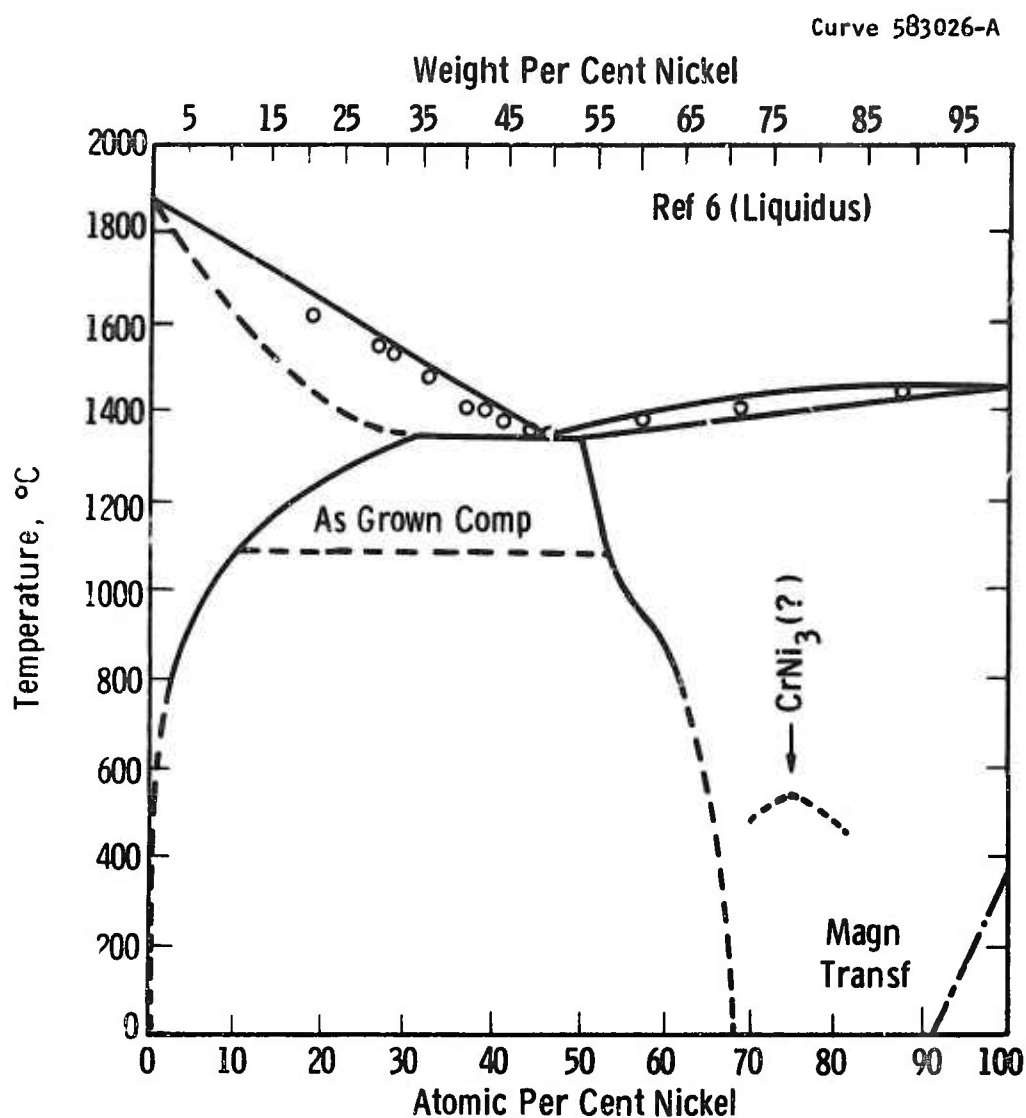


Fig. 7-Ni-Cr phase diagram

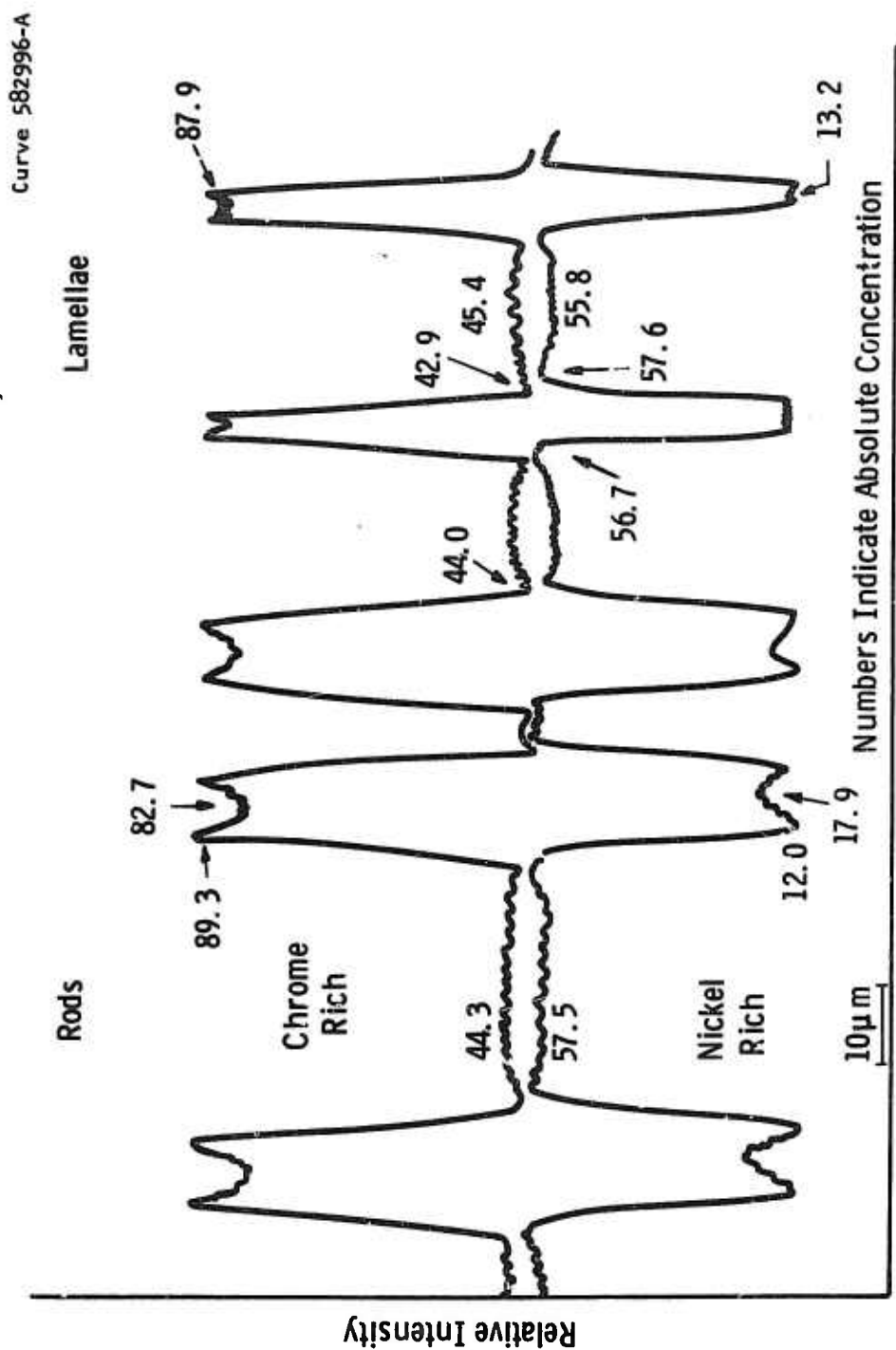


Fig. 8—Relative x-ray intensities obtained by a scanning microprobe beam. Note the sharp gradients at the Ni-Cr interphase boundary and the dips in peak centers indicating rejection of Ni from Cr solid solution

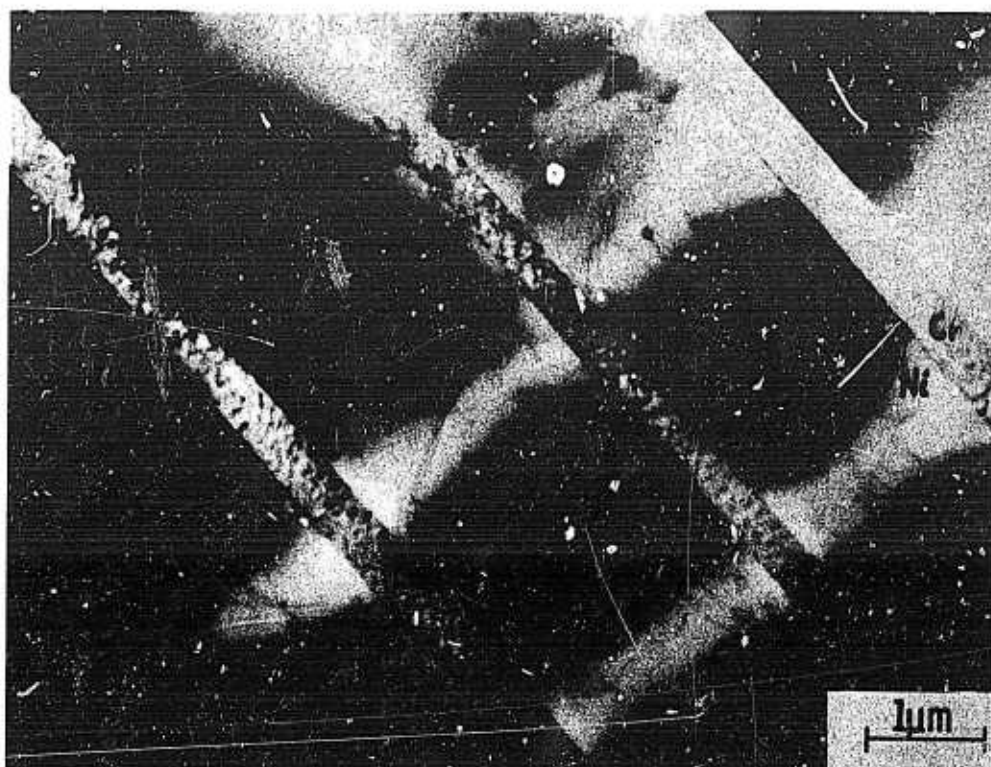


Plate NC 043

Fig. 9—A typical transmission electron micrograph of an as-grown specimen, solidified at the rate of 1/3 in./hr. All subsequent specimens shown in the Figures were grown at this rate



Plate NC 042

**Fig. 10**—High magnification electron micrograph of a typical chromium rich lamella. The internal structure was identified by electron diffraction as  $\text{Cr}_2\text{O}_3$  in the main

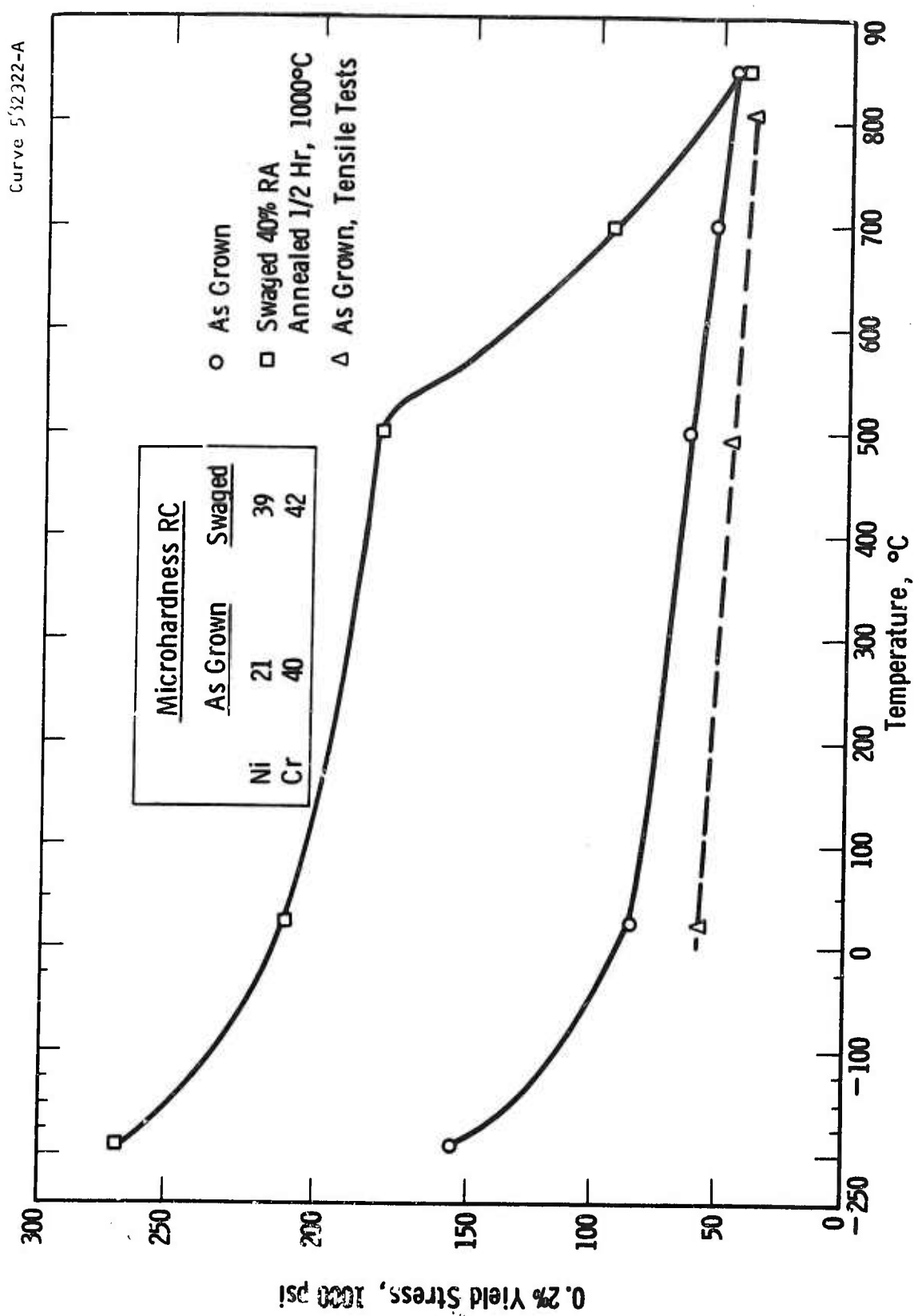
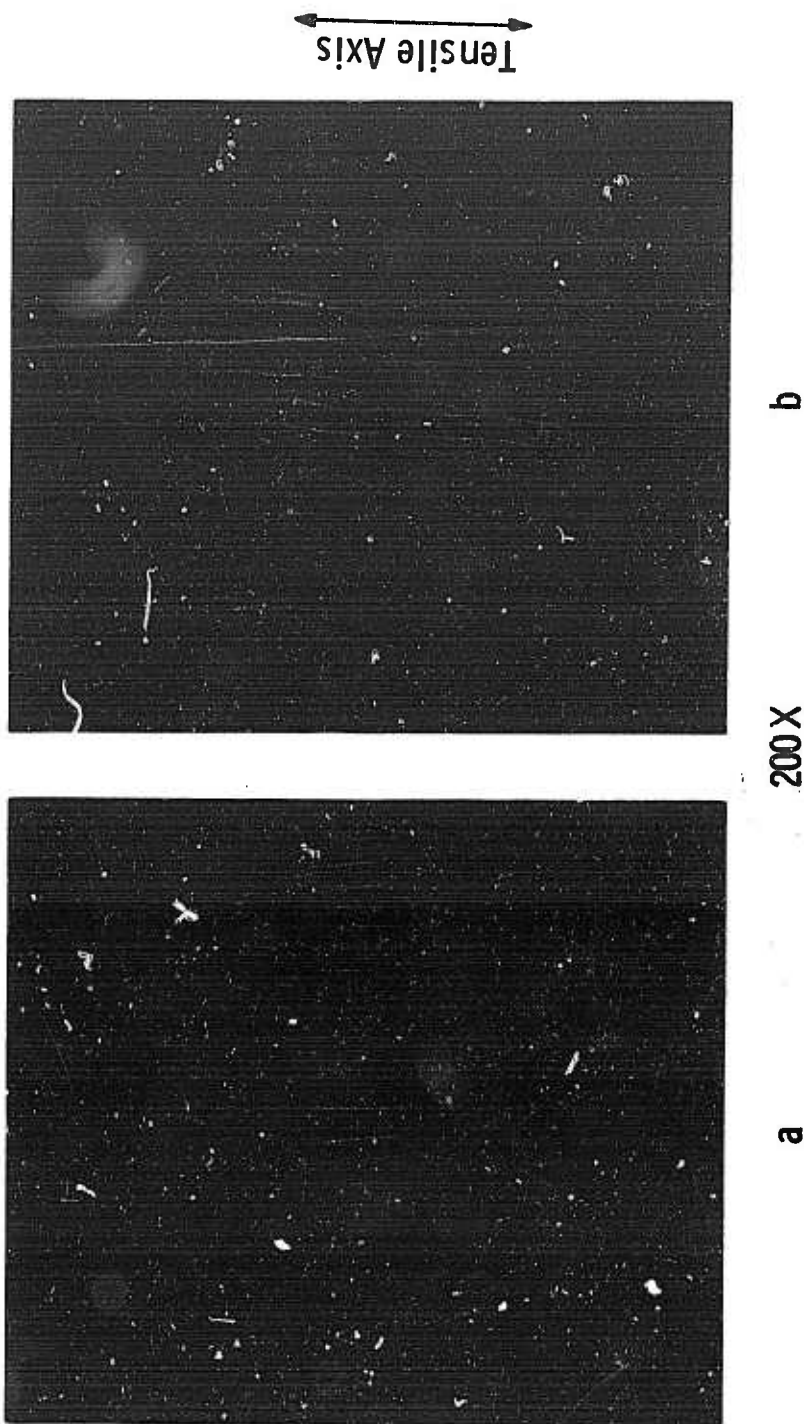


Fig. 11-0. 2% yield in compression and tension for as grown material as a function of test temperature, and compressive yield for 40% RA swaged material



**Fig. 12—Light micrograph of a longitudinal section from a specimen deformed at room temperature (1000X). Note brittle failure of the chromium rich lamellae**



**Fig. 13**—Light micrograph of a specimen deformed in tension at 500°C (200X)  
a: shoulder section  
b: gauge section. Note some ductility in the chromium rich lamellae



**Fig. 14—A specimen deformed at 800°C.  
Note increased ductility of the chromium rich  
phase and separation along the interphase  
boundary**

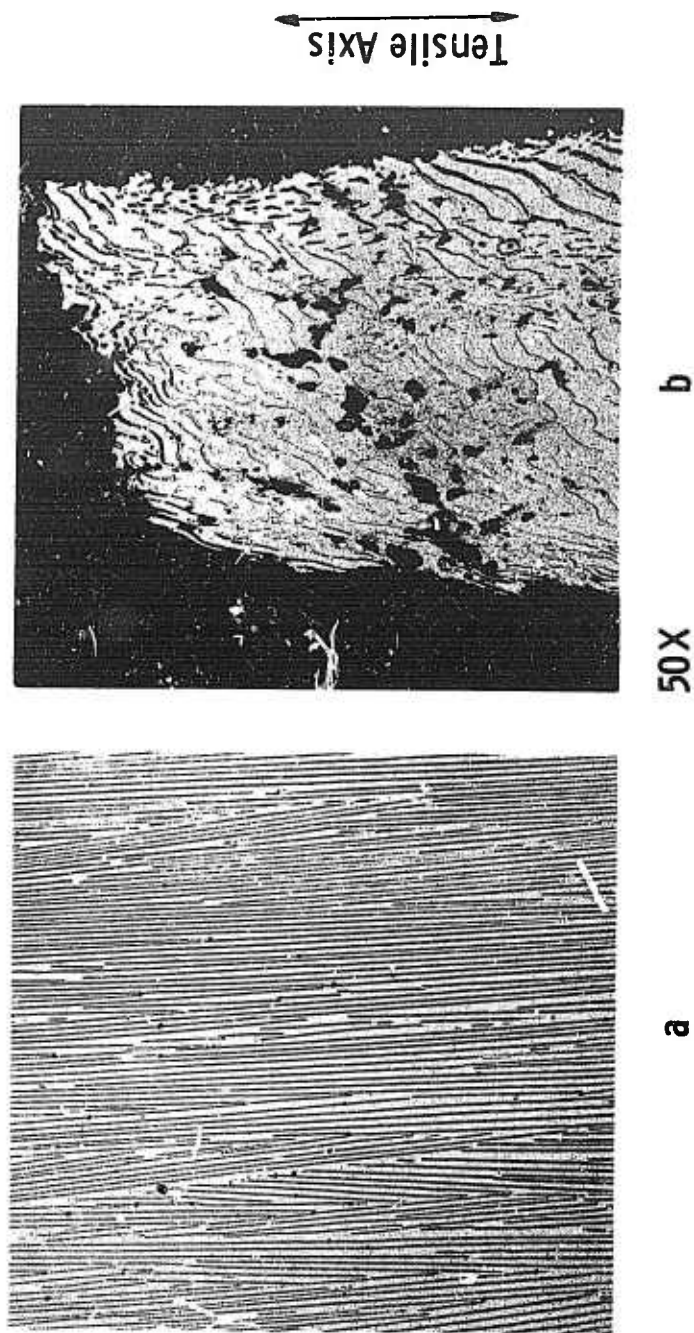


Fig. 15—Shoulder and gauge sections of a specimen, deformed in tension at 1080°C. The chromium rich lamellae are highly ductile and there is extensive void formation

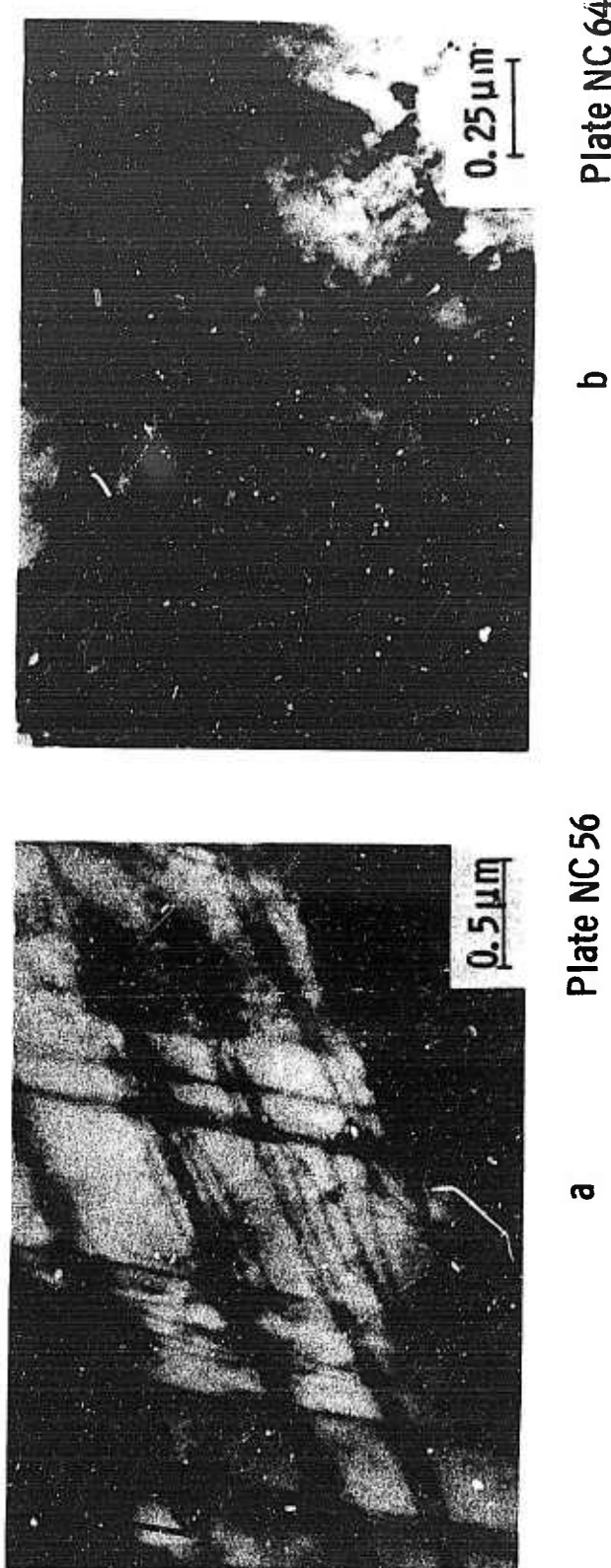


Fig. 16—Transmission electron micrograph of specimens a) deformed 2% in compression. This band structure is typical of fcc alloys with low stacking fault energy, and b) swaged 40% RA, annealed 1/2 an hour at 1000°C. Note the formation of a dislocation sub-structure. The plane of foils is (211) Ni

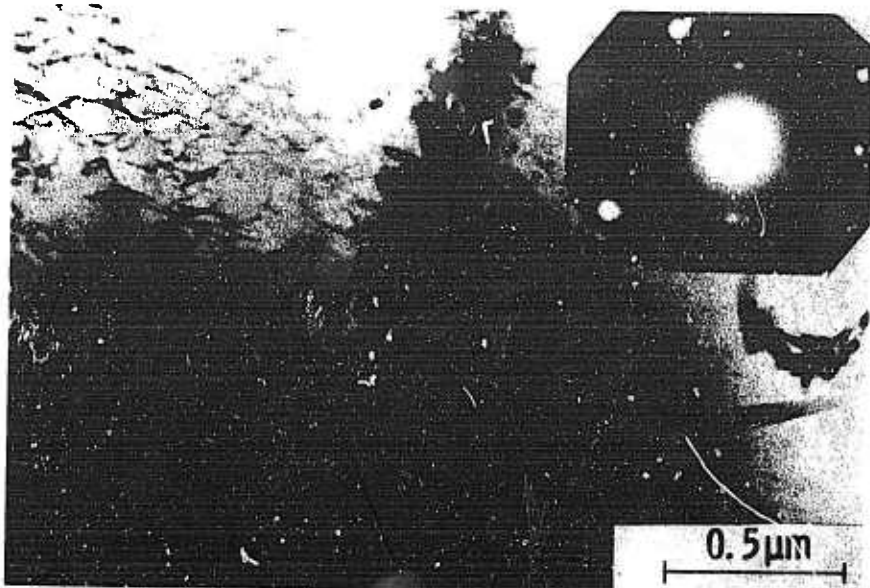


Plate NC 214

Fig. 17—Transmission electron micrograph of a specimen deformed 5% at 850°C showing dislocations and some additional particles. The diffraction pattern of this area shows (211) Ni and also  $\text{Ni}_2\text{O}_3$

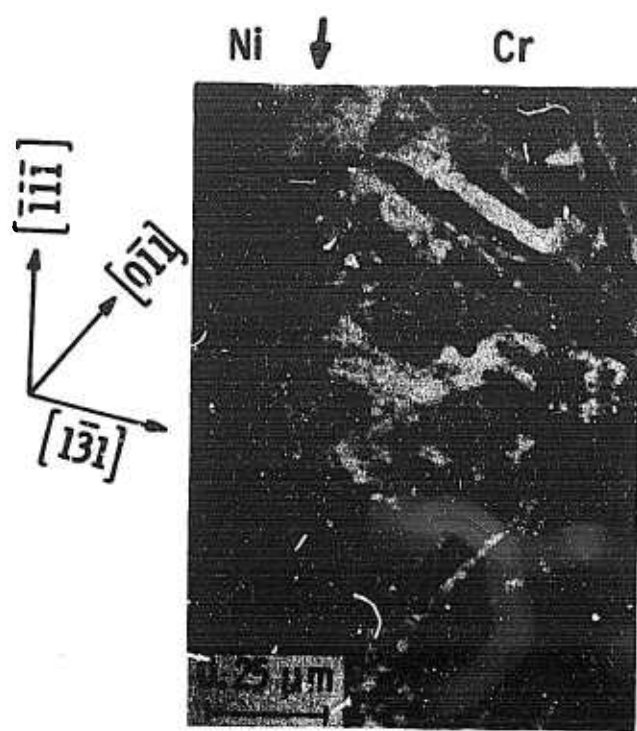


Plate NC 314

**Fig. 18**—This specimen was deformed 5% in compression at room temperature. Note the narrow dislocation band at the Ni-Cr interphase boundary (arrows)

2. Solidification Studies

by

H. D. Brody  
University of Pittsburgh

Introduction

The solidification studies are primarily concerned with understanding the fundamental parameters controlling the solidification of two phase composite materials. We will investigate the following areas.

- 1) What parameters control the stability of a planar solid-liquid interface during the directional solidification of a two phase composite? The requirements for normal freezing and zone refining will be compared.
- 2) Is there an *a priori* technique for determination of the effect of a third component on the stability of a planar interface in a two phase composite?
- 3) What parameters are critical to the spacing and the shape of the phases in a unidirectional composite?

Previous workers, in general, have worked with low melting materials, whereas the present investigation will be concerned with relatively high melting materials such as nickel-chromium. Thus, in the course of the investigation, modifications in customary techniques and controls will be required.

The approach will be from two points of view.

- 1) A fundamental mathematical modeling of the solidification process and
- 2) An empirical analysis of alloys solidified over a range of binary and ternary compositions and over a variety of growth conditions.

#### First Phase of the Study

In the first phase of the investigation we are preparing nickel-chromium alloys of eutectic and hypereutectic (chromium rich) compositions. These are being zone melted and solidified in an electron beam floating zone unit. A wide variety of growth conditions will be used and the structure will be analyzed metallographically. In this way the operating conditions, peculiar to our apparatus, necessary to maintain a planar interface will be empirically determined. To transform the results into generally applicable growth parameters, the actual thermal and interface conditions resulting from these operating conditions will be determined analytically. The empirical results will be compared to results of mathematical simulation.

Hypereutectic Ni-Cr composites are appealing in that

- 1) The volume fraction of the chromium phase can be increased.
- 2) For the same platelet spacing (nickel plate thickness plus chromium plate thickness) the thickness of nickel plates will decrease.

- 3) The corrosion resistance is expected to increase.

Mathematical Simulation of Solidification

The platelets (or rods) in a two phase alloy can be expected to grow perpendicular to the solid liquid interface. For unidirectional freezing at a planar interface, platelets would be parallel and unidirectional. If the interface becomes microscopically rough or cellular, the platelets will curve and become discontinuous. Conditions for a stable interface in normal freezing of a two phase alloy have been treated in some detail by Jackson<sup>1</sup> and by Flemings.<sup>2</sup> The simpler development of the latter indicates the interface will be planar if the actual temperature gradient,  $G$ , at the interface is greater than the gradient in liquidus temperatures of the melt  $\frac{\partial T}{\partial X}$  at the interface, i.e.,

$$G > \frac{\partial T_L}{\partial X} \quad (1)$$

For an alloy of composition  $C_0$  freezing in the  $X$  direction at a growth rate of  $R_x$ , as shown in Fig. 1, this criterion becomes

$$\frac{G}{R_x} \geq \frac{m(C_E - C_0)}{D_L} \quad (2)$$

where  $C_E$  is the eutectic composition,  $m$  is the slope of the liquidus at  $C_E$  and  $D_L$  is the diffusion coefficient in the liquid. Steep thermal gradients and slow growth rates favor a stable planar interface. Except for thermal undercooling, this simple treatment ignores a possible

breakdown of the interface for a pure binary alloy right at the eutectic composition. Convection decreases the stability of the interface.

Zone melting is more commonly used than normal freezing for high temperature material. The growth conditions imposed by the stability criterion (equation 1) is expected to be different in zone melting than for normal freezing, (equation 2). The common assumption made for zone melting and freezing is that at steady state the composition within the liquid zone is uniform. Such a simple assumption leads to the conclusion, see Fig. 2, that any positive thermal gradient at the solidifying interface will be sufficient to maintain a planar interface. If this were true, the only problem, and one readily solved by numerical analysis, would be determining the length of the transient. In this simple scheme convection would favor a planar interface.

A closer look at the mass transport required by this simple model confounds the issue as no steady state condition is apparent. At steady state, solute would be rejected at the solidifying interface at a rate  $(C_E - C_0)R_x$  grams per sec as shown in Fig. 2d, and solute would be required at the melting front. In the absence of convection there must be a concentration gradient to move the solute across the liquid zone. If the same amount of solute is required at the melting interface as is rejected at the solidifying interface, then there can be no composition gradient. On the other hand if there is a concentration gradient, some solute must diffuse into the solid, a slow process, or

the liquid must be enriched. A steady state condition in the absence of convection is not apparent. Will the solute content in the liquid zone oscillate and lead to periodic breakdown of the interface during growth? A closer analysis of the melting interface and of the effect of convection will be attempted during the next contract period.

#### Experimental Work

Initial work has been concerned with assembly of apparatus for electron beam floating zone melting, for induction melting and directional solidification, and for alloy preparation. We have been gaining familiarity with the electron beam unit and the range of operating parameters required to maintain a stable liquid zone in nickel chromium eutectics. Examples of the microstructures obtained on two tenths inch diameter rods of nickel chromium eutectic alloy, obtained from Dr. W. C. Johnston of Westinghouse, are shown in Figs. 3a and 3b. Initial results indicate that the electron beam is a promising tool for growing Ni-Cr eutectic composites.

An initial difficulty encountered with the apparatus is illustrated in Fig. 3b. The mechanism that drives the electron emitter, a tungsten filament, was sticking periodically due to a coated and misaligned gear. As a result the solid liquid interface was periodically accelerated and decelerated. This led to simultaneous breakdown of the platelets at intervals corresponding to the frequency of sticking. This structure would clearly be weak as the platelets all terminate in the same

transverse plane. The sticking of the drive was verified by attaching a pen to the filament box and tracing a line on a rotating drum. Non-linearity in the line verified the unevenness of the filament motion. This situation was corrected, the uniformity of drive verified, and a new Ni-Cr eutectic sample grown, which is currently being prepared for metallographic analysis.

An apparatus has been assembled for casting rods which are of the hypereutectic and eutectic compositions. A charge of the desired composition will be induction melted in argon. Vacuum will then be used to draw samples up into mold tubes dipped into the melt.

In future experiments we will grow Ni-Cr alloys of eutectic and hypereutectic (chromium rich compositions) over a variety of growth conditions and analyze the microstructures obtained.

#### Graduate Students

Mr. Y. T. Pao is performing the experimental work for this program.

1. Jackson and Hunt: Trans. IMD of AIME Vol. 238, August 1966, pp 1129-1142.
2. Mollard and Flemings: Trans. IMD of AIME Vol. 239, October 1967.

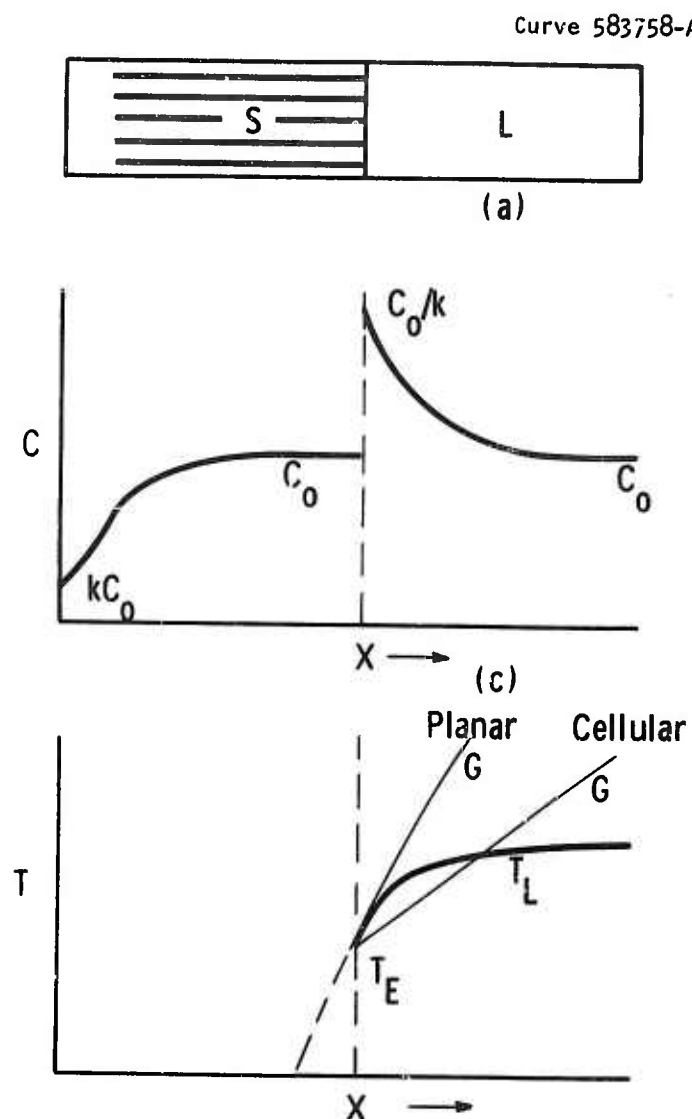


Fig. 1—Growth conditions for normal freezing of two phase composites. (a) Geometric arrangement freezing from left to right. Initial transient is first single phase then two phase increasing to the steady state volume fraction ratio of phases. (b) Concentration profile in solid and liquid phases. (c) Gradient in liquidus temperature ahead of interface and actual thermal gradient showing condition for planar and rough interface

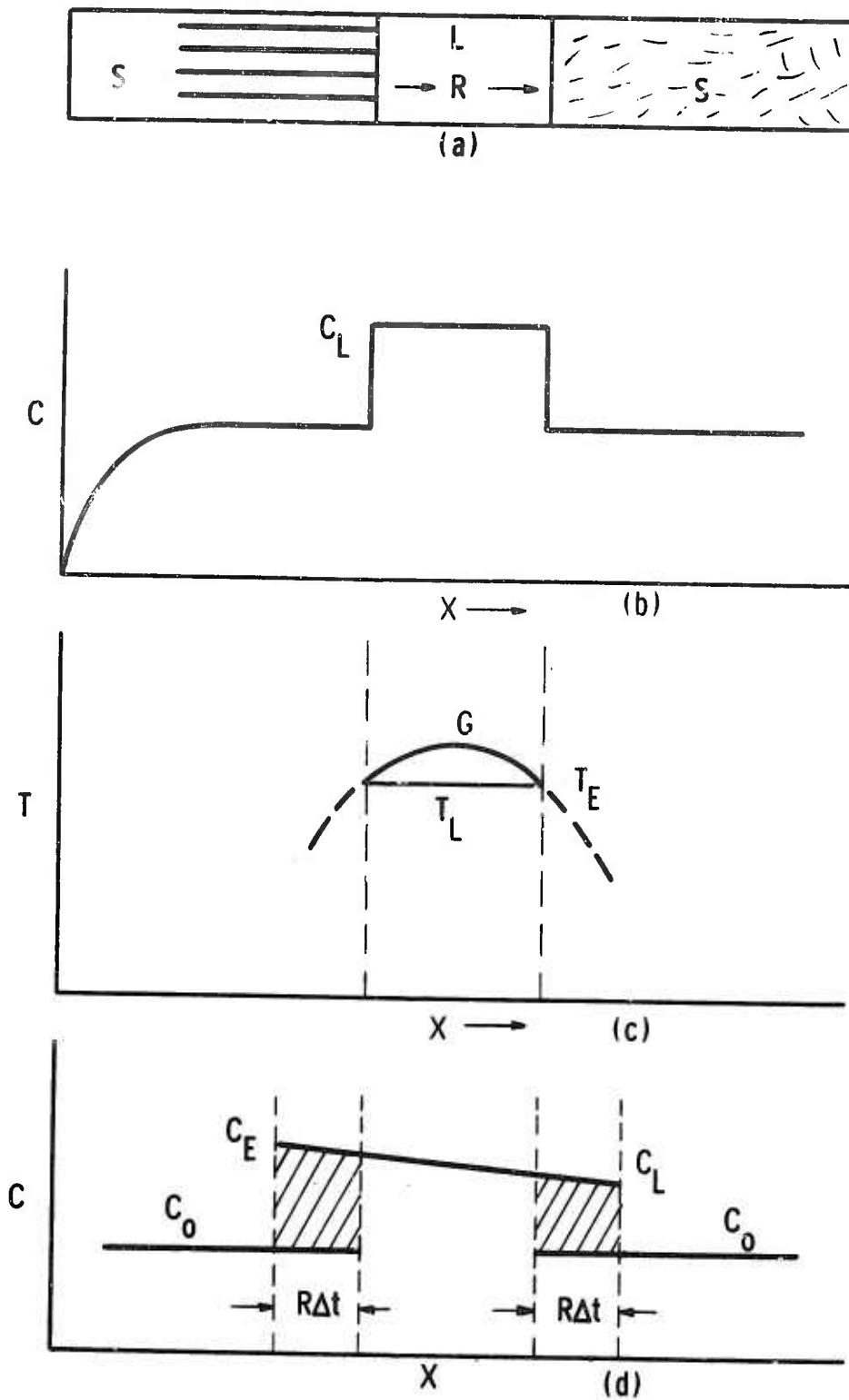
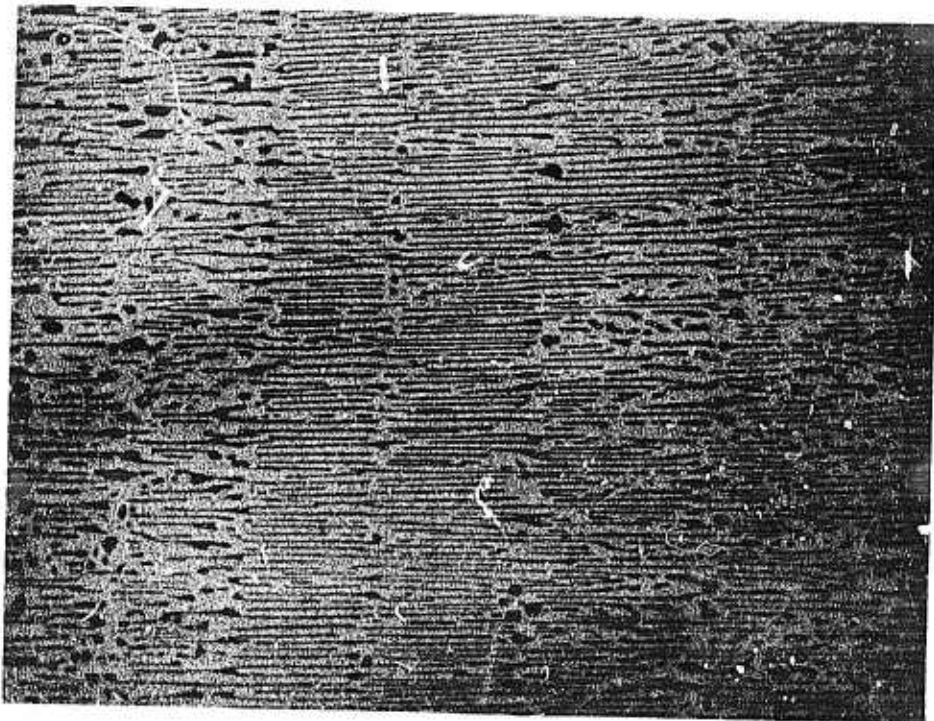


Fig. 2—Growth conditions for zone melting and freezing.  
 (a) Geometric arrangement. (b) Composition profile in liquid and solid phases. (c) Gradient of liquidus temperature in the liquid zone and actual thermal gradient. (d) Solute rejection at freezing interface,  $(C_E - C_0) R\Delta t$  and solute absorption at melting interface,  $(C_i - C_0) R\Delta t$



(a)

X 250



(b)

X 250

Fig. 3-(a) Transverse and (b) Longitudinal cross sections of the Ni-Cr eutectic grown in the electron beam unit. The discontinuous growth shown in (b) is due to variations in the interface velocity

3. The Effect of Microstructure on the Behavior of Nickel-Chromium Alloys under Conditions of Thermal Shock

by

R. D. Townsend  
Carnegie-Mellon University

The design and construction of an apparatus for studying the effects of thermal cycling in these alloys is progressing. Since the completion of this work will take some time, it has been decided to initiate the program by characterizing the thermal stability of these alloys, using the simpler experimental technique of studying the effects of temperature changes during creep. The basic creep behavior of a series of different microstructures will be studied at temperatures in the range 700°C-850°C and the effect on the creep rate, and on the rupture life, of short periods of overheating to temperatures in the range 900°C-1,000°C, will be observed.

This work should provide useful background material for the thermal cycling behavior on two counts: 1) Coffin<sup>1</sup> has found that the number of cycles to failure during thermal cycling is independent of whether the specimen is subjected to tensile or compressive stresses at the highest temperature. Thus the effect of periodic overheats on the creep behavior of an alloy may be directly relatable to the behavior of the material under normal thermal cycling conditions. 2) Rowe and Freeman<sup>2</sup> have observed no marked increase in the creep rate at 816°C of a M-252 nickel-chromium alloy when subjected to periodic overheats at 1093°C, but did observe increases in the ductility and in the rupture life. These

changes were thought to be due to metallurgical effects, but these have not been specifically identified. Since the purpose of this investigation is primarily concerned with the effects of microstructure on thermal cycling, the stability of different microstructures under these conditions is something which should be investigated at an early stage. Work is currently progressing on the building of a creep rig and on the preparation of specimens for this part of the investigation.

1. L. F. Coffin, Trans. ASME Vol. 79, No. 7, pp. 1637, 1957.
2. J. P. Rowe and J. W. Freeman; N.A.C.A. Tech. Note 4224, 1958.

4. Low-Cycle Fatigue of Niobium Single Crystals

by

J. C. DiPrimio  
University of Pittsburgh

Introduction

Most detailed fundamental studies of fatigue damage have been made on face-centered cubic materials whereas many of the metals and alloys which give promise for high temperature use have a body-centered cubic structure. It has been decided therefore to concentrate on fatigue in single crystals of niobium which is b.c.c. and melts at 2470°C. The fatigue hardening behavior in the low cycle range will be studied, using as experimental parameters orientation, strain, strain-rate and atmosphere. Work to date has been concerned mainly with the construction of the testing assembly and fabrication and characterization of niobium specimens.

Testing Assembly

The Instron Tensile Testing machine has been found to give adequate performance for low frequency fatigue tests. The upper limit of the strain rate stems from the response time of the recorder, and it is anticipated that this may be increased by the use of an x-y recorder. The Linearsyn strain measuring device has been adapted to the Instron machine and will be tested, using dummy specimens made from copper. Dummy specimens will also be used to

- (1) Test for plastic buckling, using various gauge lengths.
- (2) Test the overall performance of the machine and grips in both tension-compression and at high stress.

- (3) Test the strain gauge in both dynamic and static (constant strain) conditions.

#### Specimen Preparation and Characterization

Commercially pure niobium rods, 1/4 inch diameter, will be zone refined at approximately 9 cm/hr. Using a seeding technique, single crystals of any desired orientation can be produced on the second zone pass, yielding specimens with about 24 ppm of oxygen. It has been found that electromechanical and chemical-mechanical devices cannot produce uniform specimen gauge lengths, ab initio. It has been decided therefore to form the initial specimen shape by grinding, and finish the surface with a chemical-mechanical polish. A small tungsten-wire furnace is being constructed for the final purifying anneal treatment, 12 hours at 2000°C.

The purity level of the niobium will be assessed (a) from the electrical resistivity ratio and (b) from gas analysis by vacuum fusion. The dislocation density and distribution will be determined by two techniques, (a) by an etch-pit technique on the (111) planes and (b) by a dislocation decoration technique as developed by Vardiman and Achter.<sup>1</sup> The decoration is achieved by doping with 50 ppm carbon. The carbon doping will be accomplished by vacuum depositing carbon, and the diffusion of the dopant by heat treatment. The vacuum apparatus is currently being constructed.

#### Personnel

Mr. M. Doner is performing most of the program, but was slightly delayed by the time he devoted to preparation for the comprehensive

examination. Mr. K. Sadananda is helping with x-ray work, and is especially concerned with the specimen characterization problem.

1. Vardiman and Achter, Fall Meeting of AIME, Cleveland 1967, to be published.

5. Fatigue of Metals in a Vacuum Environment

by

H. F. Andrejasik  
University of Pittsburgh

An extensive literature survey relating to the subject "Fatigue of Metals in a Vacuum Environment" has been conducted. The literature generally shows that fatigue life is better in vacuum than in air for most of the materials investigated. The relationship between fatigue life and very high vacuum has not been clearly established. In some cases a continuous variation is found and in others a stepped variation. Thus, Ham (1963) found that for pure aluminum the fatigue life was nearly constant from atmospheric pressure to pressures of  $10^{-2}$  Torr, increasing steadily from  $10^{-2}$  to  $10^{-4}$  Torr, and was nearly constant for lower pressures.

Two mechanisms have been proposed to explain the results. One, the chemical mechanism suggests that oxygen molecules in the atmosphere combine with atoms at the base of a fatigue crack, weaken the material and thus accelerate fatigue crack growth. As the gas pressure is reduced further, fewer oxygen molecules are available to weaken the material and consequently the rate of fatigue crack growth is lower. A second mechanism used to explain increased fatigue life in vacuum is based upon a concept of cold-welding. It is proposed that at low gas pressure the new fatigue crack surface developed under tension loading is only partially contaminated because of the limited number of contaminating molecules available.



During the compression portion of the cycle, uncontaminated portions of the surfaces are brought together under pressure and direct cold-welding occurs producing an increase in fatigue life. In the case of aluminum, the previously mentioned stepped variation has been found and a great improvement in fatigue life occurred between  $10^{-2}$  and  $10^{-4}$  Torr. It is proposed that at gas pressures above  $10^{-2}$  Torr there always is a sufficient thickness of surface contamination to prevent cold-welding. At gas pressure below  $10^{-4}$  the surface contamination thickness is insufficient to prevent cold-welding during the compression part of the cycle. Between these two limits of gas pressure there is a transition range and fatigue life varies rapidly within the range.

It is clear that the exact mechanism of fatigue life in vacuum is not known. An object of this aspect of the Pitt program is to determine this mechanism. We note that in published work samples were subjected only to complete reversal of loading, i.e., tension to compression. This mode of loading makes it impossible to differentiate between the chemical and cold-welding mechanisms for improved fatigue life. Consequently, the test program conducted by Mr. Andrejasik will employ three loading modes: (a) compression-tension, (b) zero-tension, (c) tension-tension. Cold-welding effect should be apparent only under compression-tension conditions, whereas the chemical reaction mechanism should be operative in all three cases. The studies will be made from atmospheric conditions to vacuums in the range  $10^{-7}$  or  $10^{-8}$  Torr and variable frequencies will be employed. The initial investigations will

be conducted on cantilever sheet specimens of 1100-H-14 aluminum in the neighborhood of room temperature. This material was chosen because previous workers have studied it and therefore results may be compared. In the initial work temperature will be constant in order to limit the number of variables.

Thus, answers will be sought to questions of the following type:

Does a continuous or stepped variation exist between fatigue life and degree of vacuum?

Does the mode of loading influence the relationship between fatigue life and degree of vacuum?

Does the test frequency influence this relationship?

What parameters affect crack propagation:

#### Progress

The vacuum fatigue testing equipment has almost been completely designed and now is in the process of being constructed. There have been a few minor changes in the design since the last progress report. After discussing the program with various manufacturers of vacuum systems, it was decided to incorporate a Zeolite trap in the foreline to reduce the possibility of back streaming while operating the vacuum system at pressures only slightly below atmospheric conditions ( $10^2$  to  $10^{-3}$  Torr). Since standard pumping systems do not have a Zeolite trap, this type of a pumping system was considered a special order resulting in a longer delivery time. A NRC Model 3505 Portable Pumping System with a 10 cfm

Welch Mechanical Pump, Model 1376B and the special Zeolite trap in the foreline has been ordered and delivery is scheduled for December 15, 1967.

The initial material to be investigated will be 1100-H14 aluminum. A standard Krouse sheet fatigue specimen will be used. To reduce the effect of specimen preparation to a minimum, the specimens will be prepared on a Type 10-31 Tensilkut Machine using a special designed template. The Tensilkut machine is available at the University and the template has been ordered from Sieburg Industries Incorporated. With this template, it will be possible to prepare specimens consistently to very close tolerances. The delivery date for this template is November 30, 1967.

It was also decided to incorporate into the initially outlined program a study of crack propagation. This study will indicate how the three loading conditions: (a) compression-tension, (b) zero-tension, and (c) tension-tension effect the rate of crack propagation. To study crack propagation, the originally designed test chamber had to be changed slightly to provide a means of measuring the crack length. Instead of a bell jar, a piece of glass pipe will be used with a stainless steel top plate containing a viewing port. Through the viewing port, a Bausch and Lomb Stereo Zoom microscope will be used to detect the start of the fatigue crack and measure its length as the fatigue test progresses. To detect and measure the length of the crack, the surface of the fatigue specimen will require some type of metallographic polish. At present we are investigating various methods which are feasible and practical for polishing the surface of a fairly large (2" x 3") sheet fatigue specimen.

## 6. Mechanical Properties of Fine-grained, Low Porosity Ceramics

by

M. Papapietro and D. Ragone  
Carnegie-Mellon University

Empirically, it is observed that the bend strength of ceramics is increased as the grain size and the porosity are decreased. This relationship to grain size may be interpreted in terms of a Cottrell-Petch model if dislocations are free to move. The effect of porosity may be thought of in terms of the Griffith crack model. A good review of the status of the experiments and thinking in this field is given in a recent article by Stokes.<sup>1</sup>

Recent work<sup>2</sup> in the area of nuclear fuel production has shown that solgel techniques can be used to make high density oxides (especially thoria) at low sintering temperatures. These oxides have very small grain sizes, i.e., measured in hundreds of Angstroms. To use the method, a sol is first prepared, for example, by peptizing thoria produced by the steam denitration of thorium nitrate. This sol is then gelled by removing some of the water. The gels can be made in many shapes (round particles or plates) depending on the technique used for dehydration. The gel is then heated slowly to drive off the remaining water and finally sintered. Because of the extremely fine grain size in the sol and gel, this sintering is accomplished at rather low temperatures.

The sol gel technique thus seems to offer the opportunity to prepare samples of ceramics with very high density and very fine grains which could be used to extend the study of mechanical properties into an

area not previously investigated and where, hopefully, higher strengths would be observed.

The investigation to date has been concerned with the methods for producing ceramic oxides other than thoria (such as  $MgO$  and  $Al_2O_3$ ) by sol gel techniques.

1. Stokes, R. J., NBS Miscellaneous Publication 257, p. 41-63 (1963).
2. Ferguson, D. E., O. C. Dean, D. A. Douglas, "Sol-Gel Process for the Remote Preparation and Fabrication of Recycle Fuels", Proc. Intern. Conf. Peaceful Uses At. Energy 3<sup>rd</sup>, Geneva, 1964, 10, 307-15 (Published 1965).

7. Solid Solution and Precipitation Hardening of Oxides

by

J. S. Foster  
Carnegie-Mellon University

The purpose of this research is to determine what processes are involved in precipitation and dissolution of second phases in oxides and how the mechanical properties are affected by these processes. The first oxide to be studied will be MgO, and both pure and alloyed specimens will be used. Other oxide systems such as BeO and BeO alloys may be studied after the initial work is completed on the MgO systems. The experimental program is divided into two phases: a study of the defect structures and precipitation and dissolution kinetics, and a study of the mechanical properties. Both programs will include temperature, oxygen pressure, and composition as variables. The initial work will be carried out on single crystal specimens; and high density polycrystalline material will be used later. This approach should make it possible to separate the effects of the environment, alloying additions, and presence of grain boundaries on the transport, dissolution, and precipitation phenomena in oxides and to show how the mechanical properties such as creep and yield strength are affected by these phenomena.

MgO has been studied by several investigators<sup>1-5</sup> and there is little agreement on the nature of the defect structure. Either oxygen or magnesium ions may be mobile in a given environment, and there has been little effort to separate out important variables such as the role of oxygen pressure. Significant ionic conduction must occur in MgO since it has been

used as a high temperature electrolyte, and the work of Goto<sup>6</sup> shows that the transport number for ions must be nearly one. This complicates the determination of the defect structure to some degree, and it will be necessary to use at least two techniques.

AC conductivity measurements reflect both ionic and electronic transport. This technique will be used along with blocking electrode experiments. In a blocking electrode experiment the ionic conduction is suppressed leaving only the electronic portion. The electronic portion can be divided into the electron and hole contributions using the technique of Patterson.<sup>7</sup> The electronic conductivities can be related to the defect equilibria in the oxide after the method of Kroger<sup>8</sup> and this will establish the defect structure. The ionic portion of the conductivity can then be directly related to the diffusion coefficients of each species. Preliminary measurements on  $\alpha$ -AgI have been carried out using Ag as the reversible electrode and graphite as the blocking electrode. This work was used to test the apparatus and technique.

A circuit for measuring AC conductivities at high temperatures is under construction. The possibility of developing a universal reference or reversible electrode is being studied. This electrode would consist of a Pt sheet in contact with the specimen, a pure oxygen ion conductor such as  $\text{Th}_{0.85}\text{Y}_{0.15}\text{O}_{1.925}$ , and a reversible metal-metal oxide electrode. By fixing the potential of the Pt electrode with respect to the metal-metal oxide electrode, an effective oxygen potential can be established at the Pt electrode. This would give a great deal of flexibility in making the measurements and may be contrasted with the typical method of using a

metal-metal oxide electrode which establishes only a single value of oxygen potential for a given temperature.

The source of high purity MgO and MgO alloys will be W & C Spicer, Ltd. Prismatic samples large enough to provide both the defect structure and mechanical properties specimens will be obtained.

The mechanical testing apparatus is being designed and will use a low thermal inertia, graphite tube furnace for heating. Suitable fixtures for compression and for three-point bending of specimens are being considered.

It is expected that the defect structure work on MgO will be under way and that the mechanical testing apparatus will be ready to use at the end of March 1968.

One second year graduate student, Mr. Amin Degani, is currently working on the defect structure phase of this research.

1. M. O. Davies, J. Chem. Phys. 38, 2047 (1963).
2. S. P. Mittoff, J. Chem. Phys. 31, 1261 (1959); 33, 941 (1960); 36, 1383 (1962).
3. H. Schmalzried, J. Chem. Phys. 33, 940 (1960).
4. R. Mansfield, Proc. Phys. Soc. (London) B66, 612 (1953).
5. E. Yamaka and K. Sawamoto, J. Phys. Soc. Japan 10, 176 (1955).
6. K. Goto, private communication, Tohoku University.
7. J. Patterson, Ph.D. dissertation, The Ohio State University, 1966.
8. F. A. Kroger, The Chemistry of Imperfect Crystals, Wiley, New York 1964.

## 8. Properties of Refractory Metals Carbides

by

J. S. Foster  
Carnegie-Mellon University

Refractory metal carbides are potentially useful at high temperatures because of their high melting points. Titanium carbide appears to be particularly interesting since it is cubic and has sufficient active slip systems to allow some plastic deformation at high temperatures.<sup>1</sup> TiC can exist over a range of composition,<sup>2</sup> and Hollox and Smallman<sup>3</sup> have shown that diffusion is a function of composition. They suggest that the Peierls stress is also affected. Studies at the Westinghouse Astronuclear Laboratory<sup>4</sup> have shown that TiC creeps very rapidly at  $T/T_{mp} \sim 0.5$  although the mechanism of creep was not clearly established. Williams<sup>5</sup> has shown that TiC can be strengthened considerably by addition of small amounts of boron. The boron forms a precipitate which is thought to be TiB<sub>2</sub>. The precipitate forms on the {111} planes of TiC, and Venables<sup>6</sup> has proposed that the boron nucleates stacking faults in the carbide.

Very little is known about the mechanical properties and strengthening mechanisms in the refractory metal carbides. Sarian and Criscione<sup>7</sup> have pointed out that the mechanisms for creep and for diffusion are not known in ZrC and the same applies to TiC. Similarly, the mechanism of precipitation of second phases such as TiB<sub>2</sub> in TiC is not known. The slip systems of ZrC and other carbides (besides TiC) have not been determined and the role of carbide composition in determining the high temperature mechanical properties is unknown. Studies of the mechanisms of precipitation

of borides in TiC and the subsequent effects on the mechanical properties at high temperatures will be undertaken.

Samples of TiC, ZrC, and VC have been obtained and experimental work using the Berg-Barrett technique to study the dislocation distribution will begin shortly. This may lead to elucidation of the slip systems in ZrC and VC. Experimental methods for producing flat plates of the carbides by reaction of graphite and high purity metals are being considered along with methods of controlling both carbon and boron levels. The mechanical testing apparatus mentioned in the previous section would be employed in this work.

One second year graduate student, Mr. Robert Palm, is currently working in this area.

1. W. S. Williams and R. D. Schaal, J. Appl. Phys. 33, 955 (1962).
2. R. P. Elliott, Constitution of Binary Alloys, p. 232, McGraw Hill, New York, 1965.
3. G. E. Hollox and R. E. Smallman, J. Appl. Phys. 37, 818 (1966).
4. L. Fleischer, private communication, Astronuclear Laboratory, Westinghouse, Pittsburgh, Pa.
5. W. S. Williams, Trans. AIME 236, 211 (1966).
6. J. Venables, Phys. Stat. Sol. 15, 413 (1966).
7. S. Sarian and J. M. Criscione, J. Appl. Phys. 38, 1794 (1967).

9. Screening of Eutectic Combinations: Cobalt Base,  
Aluminum Base and Silver-Silicon

by

R. Kossowsky, W. C. Johnston and B. J. Shaw  
Westinghouse Research & Development Center

Some time was spent in the screening of new alloys in our directional solidification apparatus. Some of these are metal-intermetallic pairs; Ag-Si is a truly ductile matrix-brittle "metal" second phase with little mutual solid solubility; while NiCr is comparatively ductile-ductile with much solubility. We are seeking combinations of this sort to characterize the role of solution strengthening. We have also prepared two more complex alloys which may have magnetic and turbine applications.

The following new alloys have been cast, directionally solidified in the 0.2" diameter apparatus by Dr. W. C. Johnston, and then examined metallographically and mechanically by Dr. R. Kossowsky.

Table I  
Cobalt Base Alloys

<u>Alloy</u>	<u>Composition, wt %</u>				
	Cb	Cr	Ta	Fe	Co
R21	21	--	--	--	Bal
R52	13	--	--	--	Bal

Table I (cont'd)

Alloy	Composition, wt %				
	Cb	Cr	Ta	Fe	Co
R53	13	--	--	15	Bal
R30	10	10	--	--	Bal
R31	9	18	--	--	Bal
R38	18	10	--	--	Bal
R46	16	17	3	--	Bal
R51	15	20	3	--	Bal
R45	--	20	26	--	Bal
R50	--	20	25	--	Bal

The cobalt base columbium eutectic (R21) had a room temperature yield strength of 160,000 psi, dropping to 115,000 psi at 1600°F.

R38, with 10% Cr replacing CoCb eutectic, was tested at five temperatures up to 2000°F where it retained strength of 39,000 psi. Two hundred hour 1500°F sulphidation tests of R46 and R51 produced weight losses of 2.4 mg/cm<sup>2</sup>, which are close to the 2.7 mg/cm<sup>2</sup> experienced by an Udimet 500 sample run at the same time. One hundred and fifty hour, 1500°F hot corrosion performed on alloy R45 showed losses of 0.85 mg/cm<sup>2</sup> compared to 2.6 mg/cm<sup>2</sup> for a standard 80 Ni-20 Cr nichrome alloy and 1.5 mg/cm<sup>2</sup> for Udimet 500.

The remainder of the directional solidification runs in the 0.2" diameter apparatus were carried out on aluminum base alloys with additions of palladium, thorium, and lanthanum. The palladium alloy is the

period, v analog of the well known nickel strengthened aluminum alloy. It is expected that its properties and microstructure should be similar to its nickel counterpart, and the system is being screened to see if this is indeed so and if there are differences that are interesting enough to warrant further exploration. The speeds of growth were varied from 1/3"/hour to 6"/hour to produce lamella of different spacing, and the Al-Pd eutectic solidified at the higher rate showed a significant improvement in the elevated temperature strength. At temperatures above 2000°C the eutectic alloy is twice as strong as the top line precipitation hardened aluminum 7076-T6 commercial alloy.

In the larger sizes (3/8" diameter to 1-1/2" diameter) five runs were made with Ni-Cr, and, for comparison, one of Udimet 520 and also one of Ag-Si. Compression tests were made on the Udimet 520; the 0.2% offset was measured at five temperatures up to 2000°F, and is not significantly different from as-received U520. This was expected on the basis of work at United Aircraft, although it is in contrast with our experience in the simpler eutectic systems in which strength improves on directional solidification. In the Ag-Si eutectic, Dr. B. J. Shaw has found that the two phases separate completely on solidification. Although the ingot did have some fine straight lamellae, the microstructure in this first attempt was spoilt by the presence of a large number of silicon dendrites.

RESEARCH AND TECHNOLOGY RESUME		1. / / / / /	2. GOVT ACCESSION / / / / / / / /	3. AGENCY ACCESSION DR2403	REPORT CONTROL SYMBOL
4. DATE OF RESUME	5. KIND OF RESUME A. New	6. SECURITY U RPT	7. REGRADING N/A	8. RELEASE LIMITATION NL	9. LEVEL OF RESUME A. Work Unit
10. CURRENT NUMBER/CODE 6. 15.45.01.D D10 AO931 B40003		10b. PRIOR NUMBER/CODE None			
11. TITLE:					
12. SCIENTIFIC OR TECH. AREA Metallurgy, Metallography 009900		13. START DATE 6/1/67	14. CRIT. COMPL. DATE N/A	15. FUNDING AGENCY DR Other	
16. PROCURE. METHOD B. Contract	17. CONTRACT/GRANT b. NUMBER DAHC-15-67-C-0176 c. TYPE L. CS	18. DATE 06 67 d. AMOUNT	19. RESOURCES EST. PRIOR FY	20. PROFESSIONAL MAN-YEARS	21. FUNDS (in thousands)
19. GOVT LAB/INSTALLATION/ACTIVITY NAME Advanced Research Projects Agency ADDRESS Materials Sciences Office Washington, D. C. 20301		20. PERFORMING ORGANIZATION NAME Westinghouse Electric Corporation ADDRESS Churchill Boro Pittsburgh, Pennsylvania 15235			
RESP. INDIV. Dr. Robb M. Thomson TEL. 202-695-6607		INVESTIGATORS PRINCIPAL ASSOCIATE TEL. (412) 256-3535 22. COORDINATION TYPE N			
21. TECHNOLOGY UTILIZATION					
23. KEYWORDS Microstructure, Mechanical Properties, High Temperature, Fatigue, Solidification,					
24. Objective (U) - A general study of the role of <u>microstructure</u> on the <u>mechanical properties</u> of <u>high temperature</u> materials.					
25. Approach (U) - Short time tensile and compression tests, <u>fatigue</u> , <u>creep</u> and <u>thermal strain</u> tests are being performed on metals, <u>principally unidirectionally solidified</u> lamellar <u>eutectics</u> , including the NiCr eutectic, and also on <u>ceramics</u> .					
26. Progress (U) - The <u>solidification</u> characteristics for various growth conditions and the <u>mechanical properties</u> over the temperature range -250 to 850°C have been obtained for the <u>Ni-Cr eutectic</u> . The composite strength is analyzed in terms of the rule of mixtures and the interpretation is backed by transmission electron microscopy at all stages.					
Papers: Mechanical Properties of a Unidirectionally Solidified Ni-Cr Eutectic Alloy Apparatus for Unidirectionally Solidifying High Temperature Eutectic Alloys R. Kossowsky, W. C. Johnston, and B. J. Shaw Presented at Met. Soc. AIME Conference, Cleveland, October 1967.					
27. COMMUNICATIONS SECURITY <input type="checkbox"/> a. COMSEC OR <input checked="" type="checkbox"/> b. NOT COMSEC RELATED RELATED	28. / / / / / / / / / / / /	29. OSA CODE BR	30. BUDGET CODE 1		
31. MISSION OBJECTIVE / / / / / / / / / / / / / / / / / /		32. PARTICIPATION / / / / / / / / / / / / / / / / / /			
33. REQUESTING AGENCY / / / / / / / / / / / / / / / / / /		34. SPECIAL EQUIPMENT / / / / / / / / / / / / / / / / / /			
35. EST. FUNDS (in thousands) CPV + 1		36.			